THE ROLE OF TSLP IN MODULATING THE ANTI-TUMOR IMMUNE RESPONSE IN A MOUSE MODEL OF METASTATIC BREAST CANCER

by

RACHAEL BRYN ERDMANN

A thesis submitted to the Faculty of Graduate Studies of

The University of Manitoba

in partial fulfilment of the requirements of the degree of

MASTER OF SCIENCE

Department of Immunology

University of Manitoba

Winnipeg, Manitoba, Canada

ABSTRACT

Thymic stromal lymphopoietin (TSLP) is produced primarily but not exclusively by epithelial cells. It has been shown to induce the production of Th2 cytokines and inflammation in allergic disease. Since Th2 cytokines have been shown to be detrimental to the anti-tumor immune response, we hypothesized that TSLP promotes the development of a permissive microenvironment for breast cancer, which facilitates the growth and metastasis of primary tumors and that it does so, in part, by inducing the development of a Th2-mediated immune response. Using the 4T1 mouse breast cancer model, we used wild type (WT) and TSLP receptor deficient ($TSLPR^{-/-}$) mice to compare primary tumor growth, metastasis to the lungs and brain, cytokine profiles and 4T1-directed lysis. Some of these parameters were also examined in mice treated with an anti-TSLP neutralizing antibody. We showed that in $TSLPR^{-/-}$ mice, primary tumor establishment, growth and metastasis to the lungs were reduced, compared to WT mice. Unexpectedly, we observed that metastasis to the brain was increased. When mice were treated with anti-TSLP neutralizing antibody, the only significant effect that we observed was a reduction in metastasis to the lung in WT mice. We also studied TSLP expression in a human invasive breast cancer microarray (TMA). Both the normal breast epithelial cells and breast cancer cells stained positively for TSLP, but it appears that it might be more highly expressed in the breast cancer tissue. Taken together, our data support the hypothesis that TSLP promotes the development of a permissive microenvironment for breast cancer. However, the role of TSLP appears to be complex since the absence of TSLP responsiveness resulted in a greater level of metastasis to the brain.

ACKNOWLEDGEMENTS

I extend my sincerest gratitude to my supervisor, Dr. Cynthia Ellison, for allowing me to join her research team. She has been an invaluable fount of knowledge and pillar of support throughout my program and it has been a privilege to work with such a wonderful mentor. My time in her lab will not be soon forgotten.

My advisory committee, Drs. Sam Kung and Yvonne Myal, have been instrumental to my success as a graduate student in Immunology. Their suggestions, criticisms and encouragement have helped to focus this project into a viable, complete thesis.

I am indebted to the Gartner/Ellison lab – Yuriy Lissitsyn, Melanie Durston and Ezgi Ogutcen – for putting up with my quirks and questions and teaching me how to be a half-decent scientist. Your companionship made coming to work everyday a pleasure.

I would be remiss if I did not thank my colleagues in the Departments of Immunology and Pathology, particularly Marian Huebner, Susan Ness and Karen Morrow, for providing stellar academic and administrative support to me for the past three years.

I am grateful to the CancerCare Manitoba Foundation for funding this project.

Finally, words cannot express my gratitude to my friends and family for putting up with my gripes about life, grad school and Manitoba. In particular, Carolyn, Sandrine, Mark, Ivan and Neil befriended a girl from Edmonton and made Winnipeg home – for which I cannot forgive them. My family has also been a constant source of encouragement on my journey for the past three years and I could not have done this without them.

TABLE OF CONTENTS

LIST OF TABLES

LIST OF FIGURES

LIST OF COPYRIGHTED MATERIAL FOR WHICH PERMISSION WAS OBTAINED

LIST OF ABBREVIATIONS

°C	degrees Celcius
APC	Antigen-presenting cell
AD	atopic dermatitis
BBB	Blood-brain barrier
CAF	Cancer-associated fibroblasts
CCLR	Cell Culture Lysis Reagent
CNS	Central nervous system
cpm	counts per minute
CTL	Cytotoxic T lymphocyte
DC	Dendritic cell
DC-LAMP	Dendritic cell-lysosomal associated membrane protein
DSS	Dextran sodium sulfate
E:T	Effector:Target
ELISA	Enzyme-linked immunosorbant assay
ER	Estrogen Receptor
FABP7	Fatty Acid Binding Protein 7
FBS	Fetal bovine serum
G-CSF	Granulocyte-colony stimulating factor
GM-CSF	Granulocyte-Macrophage colony stimulating factor
GRB7	Growth Factor Receptor Bound Protein 7
H_2SO_4	sulfuric acid
HBSS	Hank's Buffered Salt Solution

HER2	Human Epidermal Growth Factor Receptor 2
HRP	Horseradish peroxidase
i.p.	intraperitoneal
IDO-1	Indoleamine-pyrrole 2,3 dioxygenase
IFNγ	Interferon gamma
IL-12	Interleukin 12
IL-13	Interleukin 13
IL-1β	Interleukin -1 beta
IL-4	Interleukin 4
IL-6	Interleukin 6
JAK1	Janus Kinase 1
LU	Lytic Unit
MCP-1	Monocyte Chemotactic Protein-1
MDSC	Myeloid-derived suppressor cells
mg	milligram
MHC-I	Major Histocompatibility Complex - Class I
MIP	Macrophage inflammatory proteins
ml	millilitre
mm	millimetre
N	Normal
ND	Not detected
NK	Natural Killer
NKT	Natural Killer T cell

OVA	Ovalbumin
p.i.	post-injection
PBS	Phosphate-buffered saline
pg	picogram
PR	Progesterone Receptor
RANTES	Regulated and normal T cell expressed and secreted
RT	Room temperature
s.c.	subcutaneous
SEM	Standard Error of the Mean
STAT	Signal transducer and activator of transcription
TCR	T cell receptor
TGFβ	Transforming growth factor beta
Th1	T helper cell type 1
Th2	T helper cell type 2
Th17	T helper cell type 17
T_{reg}	T-regulatory cell
TLR	Toll-like Receptor
TMA	Tissue microarray
TMB	3,3',5,5' tetramethylbenzidine
TNFα	Tumor necrosis factor alpha
TSLP	Thymic Stromal Lymphopoietin
TSLPR	Thymic Stromal Lymphopoietin receptor
$TSLPR^{-/-}$	TSLP receptor knockout

WT	Wild-type
β_2m	Beta-2 microglobulin
µci	microcurie
µg	microgram
µl	microlitre

I. INTRODUCTION

1.1 BREAST CANCER

1.1.1. CANADIAN STATISTICS

In 2012, a large scale genomic study examined 2000 breast tumor samples and found that breast tumors could be classified into 10 distinct subgroups based on the genetic profile and confirmed by multiple validation clusters, such as hazard ratio and clinical outcome [1]. This finding confirmed the heterogeneity of breast cancer as a disease that has become a significant health problem in Canada and around the world. Although both the incidence and mortality rates have been steadily declining since 1997, breast cancer accounts for 25.6% of new cancer diagnoses and 14.2% of cancer deaths in women in Canada, with no discernible geographic pattern of incidence or mortality [2]. The disease is primarily found in women 50-69 years of age; however, the highest mortality rate is found in women who are more than 80 years old [2].

1.1.2. RISK FACTORS

There are numerous risk factors associated with breast cancer development. Family history is a major factor [3]. An example of this is the observation that mutations in the tumor suppressor genes BRCA1 and BRCA2 are inherited germline mutations that influence the risk of cancer in both males and females [4, 5]. Environmental and personal factors also play a role in breast cancer development. This is supported by the observation that increased parity and breastfeeding reduce the risk for midlife-onset breast cancer [6]. In contrast, some types of hormone replacement therapy in post-menopausal women have been shown to increase breast cancer risk [7].

1.1.3. CURRENT TREATMENT OPTIONS

The treatment protocol for a given patient is dependent on the patient's age, the stage and grade of the tumor, the presence or absence of the estrogen receptor (ER) and the proliferative capacity of the tumor [8]. In any case, breast cancer is typically treated with one or more of the following: surgery, radiation therapy, chemotherapy, and hormonal therapy. The tumor subtype is the major factor that determines the level of responsiveness of the tumor to any treatment [9].

1.1.4. BREAST CANCER SUBTYPES

The major groups of breast cancer subtypes, confirmed histologically and by molecular profiling, can be described as follows: Basal-like, Human Epidermal Growth Factor Receptor 2 positive ($HER2^+$), Normal, Luminal A, and Luminal B (as reviewed by Eroles *et al*., 2012) [10]. The most recently defined subtypes have not yet been categorized into larger groups in this way.

The most aggressive form of breast cancer is the triple-negative, basal-like subtype, defined as a tumor that does not express ER, the progresterone receptor (PR) and the human epidermal growth factor receptor 2 (HER2). This subtype accounts for approximately 15% of breast cancer cases and is known for being high-risk and accompanied by a poor prognosis [11, 12]. In addition, the basal-like subtype is characterized by upregulated expression of cytokeratins [13] [14]. Clinically, patients with basal-like tumors are younger at the age of onset and have large tumors that metastasize to the viscera [11]. The 4T1 tumor model used in this study is highly invasive

and has triple-negative status, making it an appropriate model for this subtype of breast cancer [15-17].

Approximately 20% of breast cancer cases are classified as $HER2^+$ [18]. It has been shown that HER2, also known as Neu, ErbB-2, CD340 and p185, plays a role in influencing the number of tumor stem cells (SC) present in the tumor mass [19]. The high expression of the HER2 oncogene in breast tumor cells has also been shown to contribute to tumor cell proliferation, apoptosis evasion, induction of angiogenesis and metastatic cell dissemination [18]. $HER2^+$ cancer cells can be further characterized by the expression of genes near the ERBB2 locus, a *neu/HER2* oncogene located on chromosome 17, in the 17q12-21 amplicon [20]. Notably, these include ERBB2 and Growth Factor Receptor Bound Protein 7 (GRB7) [21]. HER2 is associated with aggressive behavior and a poor prognosis [18].

Normal-type breast cancer, while is defined as a molecular subtype [21, 22], has been poorly defined as a histological subtype in the literature. Nevertheless, microarray analysis has shown that normal-type tumors express non-epithelial genes. In particular, genes from adipose tissue are more highly expressed [21]. For the 6-10% of patients who are diagnosed with this subtype, these tumors tend to be small in size and have a good prognosis [23].

Luminal breast cancer comprises the majority of diagnoses and can be divided into two types: Luminal A and Luminal B [23]. Both types are defined in molecular terms as being ER^+ and/or PR^+; however, the expression of HER2 and the Ki67 nuclear protein differ [23]. Luminal A breast tumors are $HER2^-$ and $Ki67^{low}$ (<14% staining [24]), whereas Luminal B breast tumors are $HER2^+$ or $HER2^-$ and $Ki67^{high}$ [23, 25, 26]. Of the

two types of luminal breast cancer, Luminal A has the better prognosis, as the tumor is graded as low-moderate and has a low rate of recurrence. Luminal B-type cancer patients have a poorer prognosis than their A-type counterparts, as Luminal B tumors tend to have a mutated version of the p53 tumor suppressor gene. In addition, the presence of HER2 and/or Ki67 contributes to the rapidly-dividing phenotype of the tumor cells, which plays a role in the relatively larger tumor size and higher tumor grade [27].

1. 2. The 4T1 Model of Metastatic Breast Cancer

1.2.1. 4T1 Cell Line

The 4T1 cell line is derived from a mammary tumor that developed spontaneously in an $MMTV^+$ Balb/c mouse that had been foster-nursed on a C3H mother [28]. It is one of four sibling lines derived from the original 410.4 tumor. Each sibling line has different metastatic potential and different levels of drug resistance [29, 30]. 4T1 in particular carries a natural resistance to 6-thioguanine and spontaneously metastasizes to lung, liver, brain and bone of tumor-bearing mice via the hematogeneous route [29-31]. 4T1 cells are "triple negative", meaning that they do not express the ER, PR, or HER-2. Recently, it was shown that they constitutively express thymic stromal lymphopoeitin (TSLP), CXCL1, monocyte chemotactic protein-1 (MCP-1), RANTES, and macrophage inflammatory proteins 1α and 1β (MIP-1α and MIP-1β) [32-35]. Their ability to produce a combination of hematopoietic chemokines, in conjunction with granulocyte colony stimulating factor (G-CSF) and granulocyte-macrophage colony stimulating factor (GM-CSF) contributes to the development of splenomegaly, which is a consequence of the granulocytosis that develops [36]. In addition, the chemotactic properties of these

cytokines promote the infiltration of the tumor by myeloid cells [37]. 4T1 cells are resistant to cell cycle control mediated by transforming growth factor-beta (TGF-β); however, TGF-β does promote 4T1 tumorigenicity by activating genes involved in migration and invasion [38-43]. Findings from Tao and colleagues revealed that 4T1 cells secreted factors known to activate the angiogenesis and lymphangiogenesis pathways, and induce the production of both acute phase proteins and cytokines. All of these contribute to the remodeling of the tumor microenvironment [44]. These investigators also noted that the metastatic 4T1 cells showed high levels of p38 MAP kinase activation and low levels of Socs1 activation, both of which are necessary for NFκB activation and inflammation [44].

1.2.2. 4T1-12B Cell Line

The 4T1 cell line used in our study is known as 4T1-12B because it carries a stably-transfected firefly luciferase construct, making it possible to quantify metastatic cells, both *in vivo* and *in vitro* [44]. It has been shown that this does not affect either the metastatic ability or the antigenic characteristics of the 4T1 cell line [44].

1.2.3. The 4T1 Mouse Model

The model used in this study is the 4T1 mouse model of metastatic breast cancer. It is an excellent model for studying breast cancer immunology, as the disease develops naturally following the injection of 4T1 cells into immunocompetent Balb/c mice. 4T1 mammary carcinoma cells, which are syngeneic to Balb/c ($H\text{-}2^d$), are implanted subcutaneously into the mammary fat pad of a female Balb/c mouse [45]. The implanted

tumor cells are very tumorigenic, so relatively few cells are required to form a primary tumor [45]. In addition, the tumor cells are minimally immunogenic, so there is no inflammation upon tumor cell injection [45]. After implantation, the tumor cells grow into a palpable primary tumor on the abdomen and spontaneously metastasize to different sites in the mouse, along similar temporal lines to human breast cancer metastasis, i.e. first to the lymph nodes, then to the lungs, liver, brain, and bones [45]. It is relatively easy to monitor the progression of the disease by measuring the diameter of the primary tumor, and the humane endpoints for the mice are well defined. They are as follows: a measured tumor diameter between 11 and 15 mm (described in Materials and Methods on page 24) receiving treatment for tumor ulceration for more than two weeks, or the onset of morbidity (rapid weight loss and/or signs of pain).

1.3. Regulation of Anti-Tumor Immunity

1.3.1. Characteristics of the Th1/Th2 Classification of Cytokines

Immune responses are broadly characterized by the cytokines produced by activated $CD4^+$ and $CD8^+$ lymphocytes and myeloid-derived antigen-presenting cells [46]. Early in the adaptive immune response, $CD4^+$ T cells are committed to a Th1 or Th2 phenotype – a process dependent on the cytokine milieu and the strength of the received T cell receptor (TCR) signal [47]. Th1-mediated immunity in $CD4^+$ T cells, which is induced by IL-12 and IFNγ and directed by the transcription factor T-bet, is defined by the production of interferon gamma (IFNγ) and other pro-inflammatory cytokines [47-49]. Th1 immunity enhances the cytotoxic capacity of $CD8^+$ killer T lymphocytes, making this type of immune response ideal for viral infections and anti-tumor immunity

[49]. Th2 immunity in $CD4^+$ T cells is characterized by the production of interleukin-4 (IL-4) and interleukin-13 (IL-13) and is directed by the GATA-3 transcription factor [47, 49, 50]. Th2 immunity is promoted by IL-4, which activates the signal transducer and activator of transcription (STAT)-6 pathway [51-53]. As IL-4 also plays a role in B cell class switching, Th2 immunity is associated with the development of humoral immune responses, chronic inflammation and resisting extracellular pathogens [49, 54]. As discussed below in sections 1.3.2 and 1.3.3, the balance of Th1 and Th2 immunity is an important factor in determining the effectiveness of the anti-tumor immune response and consequently, the extent of tumor growth.

1.3.2. The Role of Th1 Cytokines in Anti-Tumor Immunity

Several studies supporting the importance of Th1 cytokines in enhancing anti-tumor immunity have been published in the past several years. In the late 1990s, it was shown that Th2 cytokines were able to downregulate anti-tumor immunity [55, 56] and, in mice, that Th1-dominant immunity was more effective against solid tumors than Th2 immunity [57]. Not surprisingly, natural killer T (NKT) cells that produce IFNγ are able to mediate antitumor immunity [58, 59]. Terabe *et al.* further described this phenomenon by showing that the archetypal Th1 cytokine IFN-γ was necessary for tumor regression in an unspecified mouse spontaneous tumor model [58]. Indeed, $CD4^+$ T cells were found to negatively regulate immunosurveillance by cytotoxic T lymphocytes [58]. Other studies that used STAT-6-deficient, $CD4^+$-depleted, or IL-$4^{-/-}$ mice, all of which are unable to mount an effective Th2 response, showed that these mice were resistant to tumor recurrence [58, 60]. An *in vitro* study by Thakur *et al.,* using human breast cancer cell

lines, further supported these conclusions by showing that in Th1 cytokine-rich environments, tumor growth was inhibited, and tumor cells were more effectively killed *ex vivo.* They also reported that the development of myeloid-derived suppressor cells (MDSC) was inhibited [61]. Another study using a malignant melanoma model showed that Th17 cells were associated with enhanced anti-tumor immunity, and that this phenomenon was associated with an increase in the recruitment of Th1 cells to the site of the tumor [62]. IL-12, produced by macrophages in mice, has demonstrated proinflammatory effects: it enhances natural killer (NK) and $CD8^+$ T cell activity and upregulates IFNγ production [63, 64]. These data support the role Th1 cytokines play in enhancing anti-tumor immunity in both mouse models and clinical studies [65, 66].

1.3.3. Th2 Cytokines and Chronic Inflammation in Anti-Tumor Immunity

Chronic inflammation, which can be induced by an excess of Th2 cytokines, has been shown to diminish tumor immunity by inducing the generation of MDSCs [67, 68]. MDSCs are primarily defined in mice as being $CD11b^+Gr\text{-}1^+$. Both granulocytes and monocytes are members of this group [67]. Classification of human MDSCs is generally agreed upon as $CD33^+Lin^-HLA\text{-}DR^{-/low}$, however, new subtypes are often described in the literature (reviewed by Obermajer *et al*.) [69]. MDSCs have been shown to block T cell activation and proliferation, NK cell activation and limit dendritic cell (DC) maturation in addition to polarizing the immune response towards Th2 [68]. In both humans and mice, MDSC activation is associated with immunosuppression and reduced antitumor immunity [67, 70, 71]. A study using the 4T1 model of breast cancer showed that circulating $B220^+CD11c^+$ plasmacytoid DCs induced Th2 responses and generation

of $CD4^+CD25^+$ regulatory T (T_{reg}) cells and MDSCs *in vivo* [72]. Upon depletion of the plasmacytoid DCs in tumor-bearing mice, tumor growth and metastasis to bone was reduced [72].

IL-10, a pleiotropic Th2 cytokine produced by $CD25^+CD4^+$ T_{reg} cells, has been shown to inhibit the synthesis of Th1 pro-inflammatory cytokines [73, 74]. Studies utilizing the 4T1 model of breast cancer have shown that T_{reg} cells are detrimental to anti-tumor immunity by limiting $CD4^+$ T cell infiltration into the tumor site and preventing $CD8^+$ T cell activation [75]. Another study using the 4T1 model was able to show that attenuating $CD25^+CD4^+$ T_{reg} cells enhanced anti-tumor cytotoxicity, IFNγ production and long-term survival [76]. Collectively, these data support a negative role for Th2 cytokines and T_{reg} cells in anti-tumor immunity.

1.3.4. THE ROLE OF NK- CELL- DERIVED CYTOKINES

Cytokines produced by NK cells can either enhance or inhibit tumor immunosurveillance [58]. As described in the previous section, it has been shown that Th1 cytokines play a key role in mediating anti-tumor immunity. NK cells have the ability to produce IFNγ, the cardinal Th1 cytokine, following the crosslinking of their activation receptors [77]. Studies have shown that by activating NK cells by either interleukin-2 (IL-2) stimulation or by cross-linking the activating receptor, anti-tumor activity can be increased [78]. There have also been reports showing that tumor cells secrete cytokines to escape from NK cell surveillance. Notably, both indoleamine-pyrrole-2,3-dioxygenase (IDO) and TGFβ have been indentified in breast tumor

microenvironments and have been shown to impair NK cell activity both in humans and in the 4T1 mouse model [79-81].

1.4. TUMOR IMMUNOSURVEILLANCE

Tumor cell identification *in vivo* presents a unique challenge to the immune system. Superficially, tumor cells are nearly indistinguishable from the neighboring normal tissue. In a guest blog post published in Occam's Corner by The Guardian, Cath Ennis posted a succinct metaphor to describe the immunological fight against tumor cells [82]:

> *"Briefly, killing cancer cells while leaving normal cells unharmed is like trying to win an old fashioned infantry battle in which both sides are wearing the same uniform, except some of the enemy have slightly different shaped buttons, others have slightly longer bootlaces, others have slightly lacier underwear, and all have the ability to suddenly change clothes halfway through the fight."*

The class I major histocompatibility complex (MHC-I) plays a key role in tumor immunosurveillance. MHC-I molecules are found on almost every cell in the body and present peptides 8-10 amino acids in length, derived from proteins synthesized in the cellular cytosol. MHC-I is a heterodimer composed of a highly polymorphic α-chain and a conserved β_2-microglobulin (β_2m). In humans, the classical MHC-I molecules are HLA-A, B and C. In mice, they are known as H-2K, -D and -L. Non-classical MHC-I molecules also exist as HLA-E, -F and -G in humans and as Qa and Tla in mice [83]. The classical MHC-I molecules bind intracellular peptides and interact with the T-cell

receptor (TCR) on $CD8^+$ T cells. This provides the first signal in the two-signal model of T cell costimulation in the adaptive immune response [84]. The second signal in the current model of T cell activation is the interaction of the B7 membrane protein on the surface of the antigen-presenting cell (APC) and either CD28 for activation or CTLA-4 for inhibition [85]. Studies performed in two separate mouse models, one with sarcoma and one with mesothelioma, suggest that $CD8^+$ T cells play an important role in anti-tumor immunity [86, 87]. Class II MHC molecules, heterodimers composed of an α and β subunit, are expressed only on professional antigen-presenting cells (APC) and present antigens from the extracellular environment to $CD4^+$ T cells. In humans, they are known as HLA-DP, -DQ and -DR; in mice they are known as H2-A and -E.

The antigen-specific, two-signal activation model of traditional $CD8^+$ cytotoxic T cells does not govern innate NK cells. Rather, the current model of NK cell activity suggests that naïve NK cells are educated to self-MHC-I molecules and are then regulated by activating and inhibitory receptors [88]. This model of NK development accounts for the key characteristics of NK cells that are important in anti-tumor immunity. First, NK cells freshly isolated from the bone marrow are educated, or "licensed", to recognize the classical and non-classical self MHC-I molecules present on tissues. The exact mechanism for this process has not yet been elucidated [88]. MHC-I molecules can interact with either activating receptors or inhibitory receptors on the NK cell surface [88]. Once the NK cell has been released into the periphery, the "missing-self hypothesis" states that NK cell recognition and lysis of a target cell is dependent on the absence or presence of self-MHC-I molecules on the cell surface and the balance of activating and inhibitory signals received by the cell (Fig. 1) [89, 90].

It has been shown that downregulation of MHC-I is a common occurrence in tumor cells and can occur by a variety of mechanisms in humans, for example, mutations in the HLA genes, defective HLA regulation and alterations to the peptide loading mechanism [91, 92]. Modulating MHC-I expression on the cell surface is one method of escaping from T cell-mediated cytotoxicity but does not protect against NK cell-mediated killing, lending credence to the role of NK cells in tumor immunosurveillance and tumor-directed cytotoxicity.

Immunosurveillance is a key component of the 'elimination' phase of the larger anti-tumor model known as "cancer immunoediting" (reviewed by Dunn *et al*, 2004) [93]. The immunoediting model describes three phases of immune interactions with proliferating tumor cells: elimination, equilibrium and escape. The elimination phase is characterized by classic immunosurveillance, where the innate and adaptive arms of the immune system work in concert to eliminate tumor cells. If the tumor is not completely eradicated, it moves into the 'equilibrium' phase of the immunoediting model, where the tumor cells become chronically maintained and may develop variants that are not detected by the activated immune cells. These variants then enter the 'escape' phase of immunoediting. In the escape phase, the tumor has developed multiple methods of escape from the immune system and undergoes unchecked growth, resulting in a clinically detectable tumor [93].

1.5. THYMIC STROMAL LYMPHOPOIETIN

1.5.1. PROTEIN STRUCTURE AND EXPRESSION

Thymic stromal lymphopoietin (TSLP) is an IL-7-like cytokine that was first characterized in 1994 [94, 95]. It is 121 amino acids in length, with a four-helix bundle structure. It carries three potential N-glycosylation sites and has 7 cysteine residues [94]. In mice, the *Tslp* gene is located on chromosome 18, whereas in humans, it is located on 5q31, close to the cluster of cytokine genes that are important in atopic disease [94]. The human and mouse forms of TSLP, share only 43% amino acid sequence identity but a high degree of functional similarity [96, 97]. Epithelial cells produce the majority of TSLP. Gastrointestinal and thymic epithelial cells secrete TSLP constitutively. TSLP expression is inducible in epithelial cells from the skin, lungs and tonsils [98]. Within the lungs, airway smooth muscle cells are also constitutive producers of TSLP [99]. Suprabasal skin keratinocytes present in both acute and chronic lesions in patients with atopic dermatitis (AD) strongly express TSLP; however, TSLP expression is absent in normal keratinocytes [98]. While not generally produced by endothelial cells or hematopoietic cells, TSLP has been shown to originate in both mast cells and dendritic cells [98, 100]. The mechanisms involved in the regulation of TSLP expression have not been fully elucidated, but there is evidence to suggest that it is produced upon injury, toll-like receptor (TLR) ligation by microbial byproducts, and in response to other cytokine signals [101].

1.5.2. TSLP RECEPTOR

The TSLP receptor (TSLPR) is a heterodimer of an IL-7 receptor-α-chain (IL-7Rα) and a TSLP-specific γ-chain (Fig. 1) [102]. The heterodimeric structure bears homology to other receptors in the hematopoietin family but there are some notable differences [103]. TSLPR carries the conserved box1 sequence that regulates Janus Kinase 1 (JAK1) in other cytokine receptors, but lacks the conserved box2 sequence and has a single tyrosine residue located 4 residues from the carboxy terminus [102]. TSLPR has a modified WSxWS motif and multiple N-linked glycosylation sites, which indicate similarity to the Type I cytokine receptor family [104]. TSLPR mRNA has been detected in most immune cell types (DC, T cells, B cells, mast cells, NKT cells and monocytes) as well as in heart and skeletal muscle, kidney cells and in liver tissue (Fig. 2) [98]. The signaling cascade for TSLPR was not fully elucidated until recently. It was known that TSLPR signaled through STAT5, but the cognate signaling kinase was unknown [105]. It was later discovered that the heterodimeric state of TSLPR allowed for STAT-5 activation through both JAK-1 in association with the IL-7Rα subunit, and JAK-2 in association with the TSLPRγ subunit [106]. Indeed, TSLP-TSLPR signaling uses different STAT combinations depending on the cell. For example, STAT-1 and STAT-5 are activated in CD4+ T cells[107] but STAT-1,3,4,5,6 are activated when TSLP stimulates myeloid dendritic cells (mDC) [108]. This particular transcription factor activation pattern is responsible for the downstream events in TSLP-responsive cells.

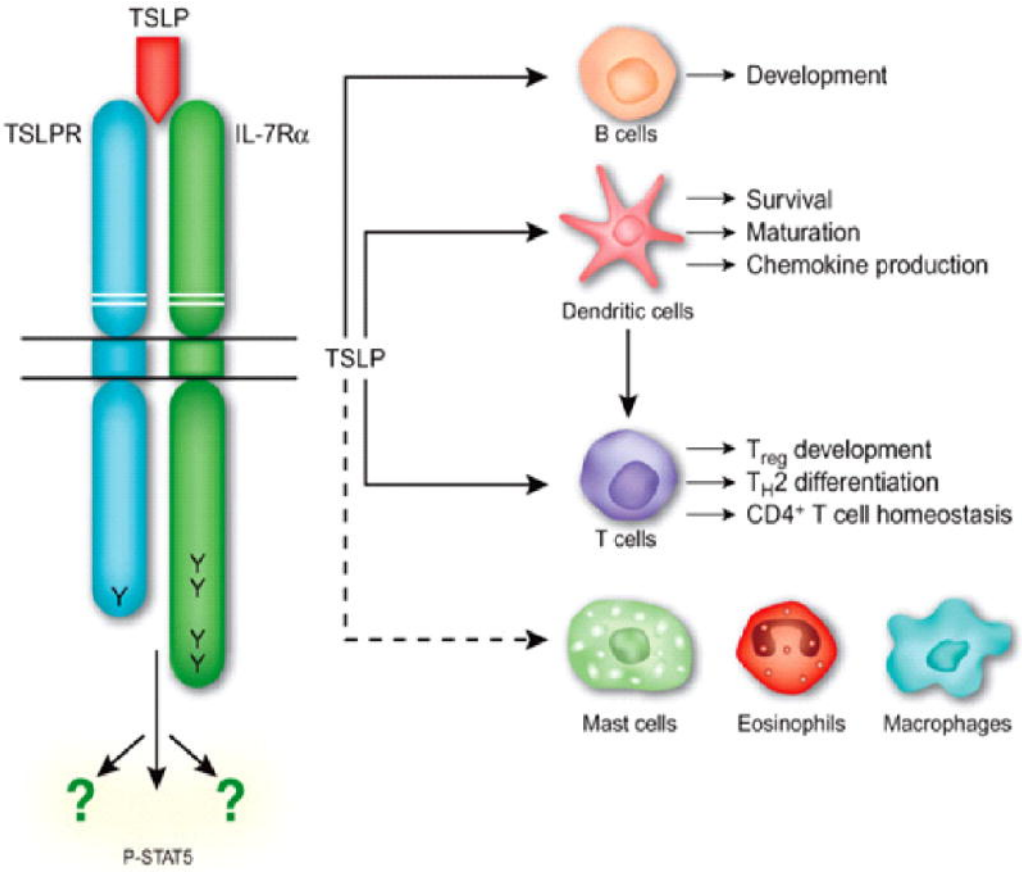

Figure 1. Structure of the mouse heterodimeric thymic stromal lymphopoietin receptor (TSLPR), composed of an IL-7 receptor α chain and TSLP-specific γ chain, and the immunological cellular targets. Reprinted by permission from John Wiley and Sons, Inc. Annals of the New York Academy of Sciences [97], 2010.

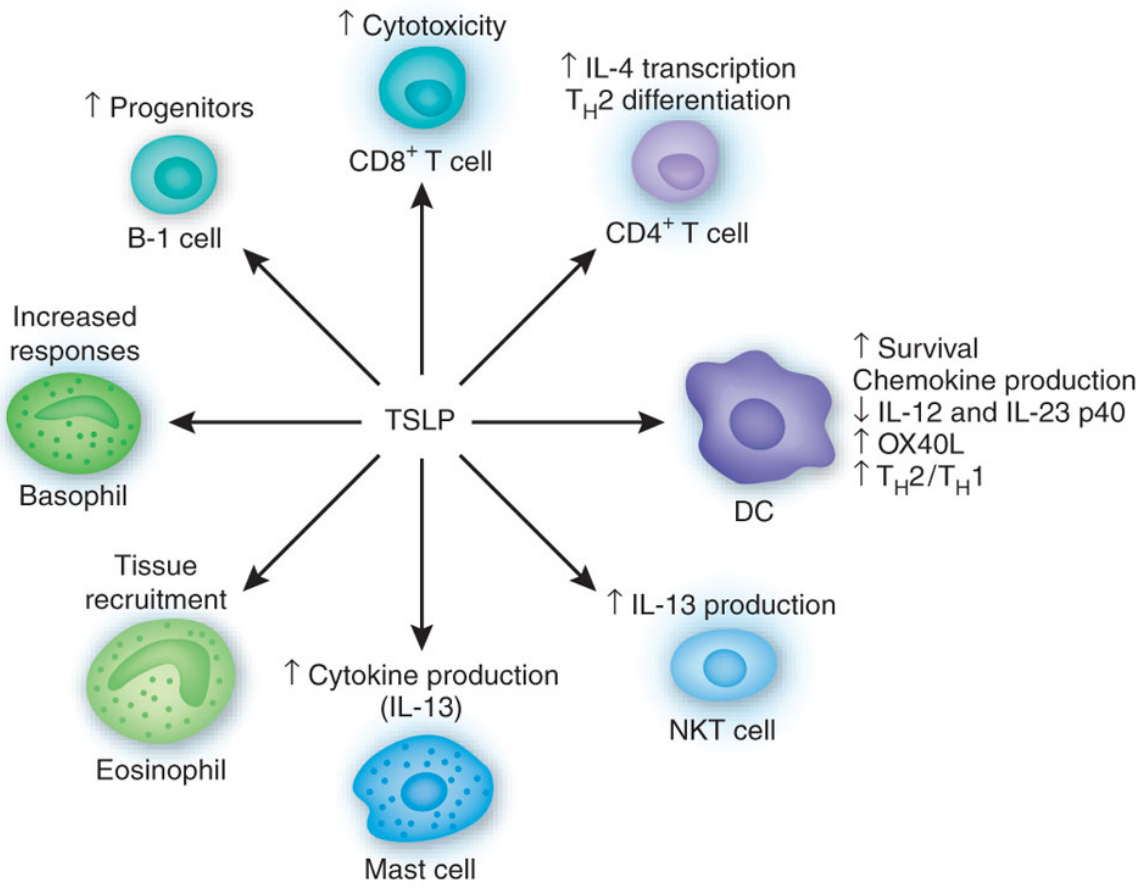

Figure 2. Pantheon of TSLP-responsive cells in mice. Reprinted by permission from Macmillan Publishers Ltd: Nature Immunology [109], 2010.

1.5.3. TSLP FUNCTION

In both humans and mice, TSLP has been shown to play a role in the activation of dendritic cells activation and the costimulation of mast cells, as well as the development of T cells. In mice, TSLP plays a role not only in T cell activation but also in B cell development [110, 111].

In dendritic cells, the complex interplay of STAT transcription factors and downstream activation of NF-κB leads to upregulation of the surface molecules CCL17, CD40, CD54 CD80, CD86, class II MHC, dendritic cell-lysosomal associated membrane

protein (DC-LAMP) and OX40L [112, 113]. Of these, it has been shown that both CCL17 and OX40L play a role in driving Th2 differentiation [110]. Interestingly, in the absence of IL-12, DCs that have been activated by TSLP, and thus express OX40L, induce naïve $CD4^+$ T cells to express an "inflammatory Th2" profile consisting of IL-4, IL-5, IL-13 and tumor necrosis factor – alpha (TNF-α) but not IL-10 [98].

In $CD4^+$ T cells, direct TSLP signaling through TSLPR combined with TCR stimulation results in increased proliferation, further Th2 differentiation, increased IL-4 transcription and increased surface expression of TSLPR, thus polarizing the immune response to Th2 [110, 113, 114]. In addition, there are no Th1 polarizing cytokines such as interleukin-12 (IL-12), TNF-α, interleukin-1β (IL-1β) or interleukin-6 (IL-6) produced [112]. A distinct absence of IL-10 and IFN-γ has also been noted when TSLP-activated DC stimulate $CD4^+$ T cells [46].

1.5.4. The Role of TSLP in Allergic Inflammation

TSLP has been heavily studied in the field of asthma and allergic inflammation. It has been implicated in the "atopic march", which is the inflammatory disease trio of atopic dermatitis (AD), asthma and allergic rhinitis, which tend to appear together in some patients [115].

Keratinocytes present in acute and chronic lesional skin of AD patients strongly express TSLP but keratinocytes in non-lesional or normal skin do not [98]. A study done by Yoo and colleagues in 2005 showed that overexpression of TSLP in the skin induced an AD-like phenotype in mice [116].

Similarly, TSLP is both necessary and sufficient to induce Th2 cytokine-driven allergic asthma in the dust mite model of allergic asthma[117]. *In vivo* studies involving airway smooth muscle cells in mice have also shown a positive feedback loop between IgE and TSLP expression [118]. Furthermore, mast cells express TSLP in response to IgE crosslinking, leading to a vicious cycle of allergy and inflammation in the lungs [98]. TSLPR-deficient mice are resistant to induced allergic asthma, but this phenotype can be rescued by administering $TSLPR^+$ T cells [119]. In addition, administering specific antigens such as mouse serum albumin (MSA) or ovalbumin (OVA) to the lungs in the presence of TSLP leads to immediate disease onset in mice [120]. These findings are consistent with clinical data showing that TSLP concentrations in the lung correlate positively with increased disease severity and increased production of Th2 chemokines [121].

In contrast to its role in airway inflammation, TSLP is expressed constitutively throughout the gastrointestinal tract and is important for maintaining intestinal homeostasis [98, 109, 122, 123]. By inhibiting proinflammatory cytokine production, TSLPR signaling is crucial for protection against helminth parasites [123]. In dextran sodium sulfate (DSS)-induced models of murine colitis, mice deficient in TSLPR were shown to have an increase in gastrointestinal inflammation compared to intact mice [123].

Collectively, these studies show the importance of TSLP as a regulatory cytokine in different systems and diseases. Some investigators have gone so far as to classify TSLP as a “master switch” for immune regulation in the context of certain diseases [124].

1.5.5. THE ROLE OF TSLP IN THE PATHOGENESIS OF CANCER

There is evidence from studies in human pancreatic cancer and mouse B16 melanoma to suggest Th2 cytokines downregulate anti-tumor immunity [55, 56]. Studies have shown that mice deficient in STAT6, a transcription factor necessary for Th2 polarization, are resistant to tumor growth and spontaneous recurrence [58] and have enhanced anti-tumor immunity against 4T1 mammary carcinoma [60]. There is also evidence from studies on human melanoma to show that chronic inflammation is a key factor in enhancing tumor progression by inducing MDSC cells that polarize T cells in the tumor microenvironment towards Th2 immunity [125]. As a corollary, IL-1 receptor-deficient mice, which have a reduced inflammatory response, have enhanced anti-tumor immunity in a model of melanoma [68]. There is also clinical data from pancreatic cancer patients showing that $CD4^+$ Th2 lymphoid cells, which express GATA-3 but not T-bet, are associated with disease progression [126]. These observations suggest that TSLP will reduce the anti-tumor immune response, as TSLP indirectly stimulates Th2 cytokine production and drives Th2 polarization [98]. In the past two years, five independent studies on four different types of cancer were published, confirming that TSLP is associated with disease progression and has a context-dependent role in anti-tumor immunity [33, 111, 126-128].

De Monte *et al.* investigated the role of TSLP in the progression of pancreatic cancer in humans. They showed that TSLP was secreted by activated cancer-associated fibroblasts (CAF), found within resected tumor samples, and that myeloid DC could be activated by factors secreted by CAF and acquire Th2 polarizing ability. In addition, De Monte *et al.* observed that DCs similar to TSLP-stimulated DC were present *in vivo*, in

pancreatic cancer patients. The enhanced Th2 polarization resulted in more Th2-skewed CD4+ T cells, which is associated with disease progression and detrimental patient outcomes [126].

Li *et al.* found that in the lung tumor microenvironment, there was a positive correlation between TSLP levels and the number of T_{reg} cells present. They also noted that T_{reg} inhibited the anti-tumor immune response. Even though TSLP is involved in T_{reg} positive selection in the human thymus, the connection between TSLP and T_{reg} in lung cancer is still unclear [111].

Using a humanized mouse model of breast cancer, Pedroza-Gonzalez *et al*. (2011) showed that TSLP promoted breast tumor growth by enhancing the Th2 cytokine profile in the tumor microenvironment. They noted that human primary breast tumor cells secreted factors capable of inducing the Th2 differentiation marker OX40L on the surface of dendritic cells and that these dendritic cells were able to elicit inflammatory Th2 cells. In studying the human breast tumors, the authors found that the tumors secreted TSLP. They also made two different but complementary findings regarding the role of TSLP in anti-tumor immunity. Firstly, by neutralizing TSLP in a culture containing blood mDCs and breast tumor supernatant, the generation of inflammatory Th2 cells was blocked. Secondly, using a humanized mouse model, they found that there was inhibition of tumor growth by entirely blocking the TSLP-OX40L axis with monoclonal antibodies against OX40L, IL-13, TSLP, or TSLPR [127]. It is important to note that this model is artificial because immunodeficient mice were populated with hematopoietic stem cells obtained from human donors who had been given G-CSF, a drug that mobilizes stem cells from

bone marrow into the periphery and has been shown to polarize the immune system towards Th2 cytokine production [129].

Olkhanud *et al*. published their findings in 2011, which demonstrated a role for TSLP in breast cancer development and progression in the 4T1 model of mammary carcinoma. They found that human breast tumor cell lines, human melanoma cell lines, and the metastatic 4T1 mammary carcinoma cell lines express TSLP, supporting the Pedroza-Gonzalez *et al.* findings from human primary breast tumor cells. They also showed that tumor-derived TSLP, rather than host-derived TSLP, was important in promoting tumor progression. Importantly, the Olkhanud study showed that tumor progression was abrogated in mice lacking the TSLP receptor ($TSLPR^{-/-}$). This is consistent with the higher number of metastatic lesions in the lungs of tumor-bearing wild-type (WT) control mice used in this study. $CD4^{+}$ T cells were found to play a role in promoting the development of a Th2 immune response, which was especially prevalent in the lungs of tumor-bearing mice [33]. Collectively, the findings from the Olkhanud study improved our understanding of breast cancer immunology; however the precise mechanisms through which TSLP facilitates the growth and metastasis of primary tumors of the breast are still incompletely understood.

Di Piazza *et al.* published an interesting report in 2012 showing that TSLP plays a protective role against tumors in a model of spontaneous cutaneous malignancy, when mice are deficient for Notch, a transmembrane signaling molecule that is involved in inducing the organization of cells into more complex structures following cell to cell contact. This finding suggests that TSLP plays a more complex role in tumor immunology than was previously thought [128]. It further suggests that Notch signaling

might play a pivotal role in the mechanism through which TSLP regulates the development and progression of cancers that originate in epithelia.

1.6. Thesis Overview

1.6.1. Study Rationale

Breast cancer is a tumor of epithelial origin, and it has been shown that epithelial cells are the primary source of TSLP[98]. The rationale for our hypothesis, shown below, was based firstly on the observation that the 4T1 mouse breast cancer cell line produces TSLP, a finding that has since been reported by others [33]. It was based secondly on our knowledge that TSLP induces a Th2 immune response in allergic disease and that Th2 cytokines promote breast cancer development progression [75, 76, 112, 117, 121].

1.6.2. Specific Hypothesis

TSLP promotes a permissive microenvironment for breast cancer, which facilitates the growth and metastasis of the primary tumor. It does so, at least in part, by inducing the development of a Th2-mediated immune response, which likely leads to an ineffective anti-tumor response.

1.6.3. Study Objectives

The primary aim of our study was to test the hypothesis indicated above. The specific objectives were to do the following:

1. Characterize the immune response to 4T1-12B tumor cells both *in vitro* and *in vivo*.

2. Determine how the loss of TSLPR function affects the tumor establishment, growth and metastasis in the 4T1 mouse mammary tumor model.
3. Determine how the loss of TSLPR function affects the cytokine and cytotoxicity responses in the 4T1 mouse mammary tumor model.
4. Determine whether treatment with an anti-TSLP neutralizing antibody affects the establishment, growth and metastasis of the primary tumor in the 4T1 mouse mammary tumor model.
5. To examine TSLP expression in human invasive breast cancer and normal tissue using tissue microarray analysis.

II. MATERIALS AND METHODS

2.1. MICE

Wild-type (WT) female Balb/c and female TSLP receptor knockout ($TSLPR^{-/-}$) mice were used at 8-10 weeks of age. WT mice were obtained from the local colony at the Genetic Models Centre at the University of Manitoba. The $TSLPR^{-/-}$ mice used in these experiments are deficient in the TSLP receptor and have a Balb/c genetic background. As previously described, $TSLPR^{-/-}$ mice exhibit normal T and B cell development and cellularity [130]. Breeding pairs were provided by Dr. W. Leonard, National Heart, Lung and Blood Institute, Bethesda, MD, bred in the Genetic Models Center at the University of Manitoba, and used at 8-10 weeks of age. All of the experiments were performed in accordance with the standards of the Canadian Council on Animal Care.

2.2. CELL LINES

4T1-12B ($H\text{-}2^{d}$) cells [44] were obtained from Dr. Gary Sahagian at Tufts University, Boston, MA. Cells were maintained in complete RPMI 1640 culture medium (Gibco, Grand Island, NY), supplemented with 10% fetal bovine serum (FBS) (Gibco, Grand Island, NY) and 1% penicillin-streptromycin (Gibco; 10000 units/ml Penicillin, 10000 µg/ml Streptromycin).

Cells were allowed to grow to 85-100% confluence and released from the flask by rinsing with 5-10 ml 1X phosphate buffered saline (PBS) and treated with 1 ml 0.25% Trypsin-EDTA (Gibco, Grand Island, NY, USA) for 2 minutes prior to passage. They

were then washed with fresh complete RPMI and plated at 20-40% confluence. Cells were not used beyond passage 15.

The lymphoma cell line YAC-1 (H-$2^{k/d}$) was obtained from the American Type Culture Collection (Rockville, MD) and maintained in complete RPMI as described above. Cells were grown to 90-100% confluence and passaged every 2-3 days. Cells were not used beyond passage 15. YAC-1 cells were used as a positive control for the cytotoxicity assays as they are sensitive to lysis by NK cells [131].

2.3. Inducing Primary Tumors in Mice

Primary tumors were induced using the protocol established by Pulaski and Ostrand-Rosenberg [45]. Prior to induction, 4T1-12B cells were maintained as described above from the point of thaw until day -1. On day -1, 4T1-12B cells were passaged so that they reached 75-90% confluence on day 0, when they were were rinsed with 5 ml 1X PBS and released from the flask using 1ml 0.25% Trypsin-EDTA. Cells were then washed with RPMI-penicillin/streptomycin (1%) and adjusted to a concentration of 7 x 10^4 cells/ml. WT or $TSLPR^{-/-}$ mice were then injected with 100 µl of the 4T1-12B cell suspension subcutaneously (s.c.) into the right mammary fat pad to achieve a dose of 7 x 10^3 cells/mouse. Mice were then ear-punched for identification purposes. An early health check was performed within 7 days of 4T1-12B cell injection to obtain the baseline weight for each mouse. The diameter of the primary tumor growth and weight of each mouse was monitored and recorded every 3-4 days. When the primary tumor grew to approximately 9 mm^2, estimated by palpation of the injection site, electronic vernier calipers (Mastercraft, Toronto, ON) were used to obtain the tumor dimensions. If the

tumor began to ulcerate, the mouse was treated with BNP topical antibiotic (Vétoquinol, Lavaltrie, QC) to control infection and buprenorphine (Temgesic; Schering-Plough, Kirkland, QC) for analgesia.

Mice were euthanized at prescribed experimental time points or at their humane endpoints, which were defined by any of the following criteria: (1) a measured tumor diameter between 11 and 15 mm; (2) a treatment period of more than 2 weeks for ulceration; and, (3) the onset of morbidity, as demonstrated by rapid weight loss and/or symptoms of pain. Mice were sacrificed on day 60 if they had not yet reached their humane end point.

2.4. Measurement of Cytokine Expression in Naïve and Tumor-Bearing Mice

2.4.1. *De novo* Cytokine Expression

Spleens were harvested from naïve WT or TSLPR$^{-/-}$ mice and placed in RPMI/Penicillin-Streptomycin (1%). They were then minced with scissors and pressed through a #60 stainless steel mesh screen to obtain a single-cell suspension. Splenocytes were then washed once in incomplete RPMI/Pen-Strep. Cells were resuspended in complete RPMI/5% FBS and counted using the Trypan Blue exclusion method. The cell suspension was then adjusted to a concentration of 1 x 10^7 live white blood cells/ml. Concurrently, confluent 4T1-12B cells were detached from the tissue culture flask as described above and adjusted to a concentration of 1x10^5 cells/ml in RPMI/5% FBS. One milliliter each of splenocyte suspension and 4T1-12B cell suspension was added to a single well on a 24-well tissue culture plate to obtain splenocyte : 4T1-12B ratios of 100:1, 50:1, 25:1 and 12.5:1. Controls consisted of 1 ml of either splenocytes or 4T1-12B

cells plus 1 ml of RPMI/5% FBS to obtain cell concentrations equivalent to the coculture conditions. Plates were incubated at 37° C (5% CO_2) and supernatants were drawn off at 24 and 48 hours.

2.4.2. *IN VIVO* CYTOKINE EXPRESSION

Spleens were harvested from tumor-bearing mice on days 7, 14, 21, 28 and 60 post-injection (p.i.) and single cell suspensions were prepared as described above. Splenocyte cultures were incubated at 37° C and supernatants were aspirated at 24 or 48 hours to obtain maximum cytokine concentrations.

Culture supernatants were tested by Enyzme-Linked Immunosorbent Assay (ELISA) for IFN-γ, IL-4, IL-10, IL-12(p40) (BD OpEIA ELISA kit, BD Biosciences, San Diego, CA, USA), IL-13 (eBioscience ELISA Ready-Set-Go, eBioscience, San Diego, CA, USA), TNFα and TSLP (DuoSet ELISA Development System, R&D Systems, Minneapolis, MN, USA). Assays were performed according to the manufacturers protocol. Briefly, the ELISA plate was coated with capture antibody and incubated overnight at 4°C. After washing, the plate was blocked for one hour at room temperature (RT), washed, and samples were then added to the plate and incubated for two hours at RT. After another wash step, the detection antibody and horseradish peroxidase (HRP) were added and incubated for one hour. After a final wash, TMB substrate was added and the reaction was allowed to proceed for 30 minutes. After stopping the reaction with 2N H_2SO_4 (Fisher, Ottawa ON), colourimetric changes were measured by a SpectraMAX Plus microplate reader (Molecular Devices, Sunnyvale CA). Raw data was analyzed with the SoftMAX Pro software (v. 4.7.1; Molecular Devices, Sunnyvale CA).

2.5. MEASUREMENT OF 4T1-12B AND YAC-1-DIRECTED CYTOTOXICITY

A 4-hour chromium-51 release assay was used to measure 4T1-12B-directed cytotoxicity mediated by splenocytes from naïve or tumor-bearing mice. YAC-1- directed cytotoxicity was used as a positive control for the assay [132].

Spleens were harvested from naïve or tumor-bearing WT or $TSLPR^{-/-}$ mice and placed in Hank's Balanced Salt Solution (HBSS) (Sigma, Oakville, ON). Spleens were minced with scissors and pressed through a fine mesh screen to obtain a single-cell suspension and washed once in HBSS. Cells were resuspended in complete RPMI/5% FBS, and counted using the Trypan Blue exclusion method. The cell suspension was then adjusted to a concentration of 1×10^7 live white blood cells/ml. Three, 2-fold serial dilutions were prepared and plated in triplicate in a 96-well v-bottom microtiter plate.

4T1-12B and YAC-1 target cells were labeled with chromium-51 radionuclide, sodium chromate in normal saline (Perkin Elmer, Woodbridge, Ontario, Canada) at a concentration of 50 μCi/1×10^6 cells for 60 min in a 37°C water bath with constant agitation. If the chromium-51 was over the half-life of 30 days, the incubation time was extended to 75 minutes. After labeling, the target cells were washed once in HBSS and twice in complete RPMI/5% FBS. Target cells were counted and adjusted to a concentration of 1×10^5 cells/ml. One hundred microliters of target cells were added to each well containing effector cells to obtain the following four effector to target ratios (E:T): 100:1, 50:1, 25:1 and 12.5:1. One hundred microlitres of target cells were added to each of 6 wells containing RPMI/5% FBS on the microtitre plate to obtain control values for spontaneous and maximum chromium-51 release.

The microtitre plate was incubated for 4 hours at 37°C and then centrifuged for 10 minutes at 300x g. One hundred microlitres of supernatant was removed from each well and added to a 6x50mm glass culture tube. The counts per minute (cpm) were determined using a gamma counter (Wallac Wizard, PerkinElmer, Woodbridge ON). Percent lysis values were calculated as follows:

$$\% \text{ lysis} = \frac{\text{cpm (experimental) - cpm (spontaneous)}}{\text{cpm (maximum) – cpm(spontaneous)}}$$

The mean percent lysis values and SEM were calculated for each triplicate set of E:T ratio and response curves were drawn. Lytic units were calculated using exponential fit as described by Pross *et al.* [133].

2.6. MEASURING METASTASIS IN TUMOR-BEARING MICE

The lungs and brains of tumor-bearing mice were harvested, weighed and flash-frozen in liquid nitrogen prior to storage at -80°C. Frozen tissue was thawed, then lysed as previously described by Manthorpe *et al*.[134] and recommended in the manufacturer's protocol.

After thawing, the tissue was mechanically homogenized and mixed with 500 µl cell culture lysis reagent (CCLR; Promega, Madison, WI, USA). The homogenate was vortexed for 15 minutes and subjected to three freeze-thaw cycles before centrifugation for 3 minutes. The supernatant was collected and saved in a separate microcentrifuge tube. Another 500 µl of CCLR was added to the pellet and the lysing process was repeated without the freeze-thaw cycles. After the second centrifugation, the second

supernatant was collected, combined with the first supernatant and frozen at -80°C until analysis. The total protein content in the tissue lysate was determined using a Lowry protein quantification kit (BioRad, Mississauga ONT, CA).

Free firefly luciferase in the tissue lysate was measured with the Luciferase Assay System (Promega, Madison, WI, USA). Lysates were adjusted to a concentration of 30 mg/ml, which we found to be the optimal protein concentration range for obtaining the strongest luciferase signal as determined by prior optimization experiments. Duplicate samples of the lysate were diluted in CCLR in a two-fold series, on an opaque white round-bottom 96-well plate (Corning, Corning NY). One hundred microlitres of Luciferase Assay Reagent (Promega, Madison, WI, USA) was added to each well of lysates, immediately before reading. Plates were read for 2 seconds using the BioTek Synergy4 microplate reader (BioTek, Winooski, VT, USA). CCLR alone was used as the negative control, and luciferase counts were standardized against lysate from a known number of 4T1-12B cells. To determine the relative luciferase signal per organ, the raw photon/second value was multiplied by the dilution factor that was used to achieve a protein concentration of 30 mg/ml. To correct for background chemiluminscence in the tissue, we subtracted the mean chemiluminescent signal emitted by lung or brain tissue harvested from healthy WT or $TSLPR^{-/-}$ control mice.

2.7. DETECTION OF TSLP EXPRESSION IN NORMAL HUMAN BREAST TISSUE AND HUMAN BREAST CANCER SAMPLES

Tissue microarrays (TMA) were prepared using samples from the Manitoba Breast Tumor Bank, which operates with the approval of the Faculty of Medicine, University of Manitoba, Research Ethics Board[135]. Fifty normal epithelium and 50 breast cancer core tissue samples (0.6 mm diameter) were taken from selected areas using a tissue arrayer instrument (Beecher Instruments, Silver Spring, MD). Serial sections of TMAs were de-waxed, rehydrated and submitted to heat-induced antigen retrieval for 8 min, in the presence of citrate buffer using an automated tissue immmunostainer (Discovery Staining Module, Ventana Medical Systems, Tucson, Arizona). Immunohistochemical staining for TSLP using anti-human TSLP antibody (ab79493; Abcam, Cambridge, MA) was done as described elsewhere[136] using a dilution of 1:100.

2.8. TREATMENT WITH MOUSE ANTI-MOUSE TSLP ANTIBODY

A mouse anti-mouse-TSLP neutralizing antibody (muM702) [123], was provided by Amgen, Inc. The antibody consists of the rat anti-mouse TSLP F(ab) region of the M702 clone, conjugated to the mouse IgG1heavy chain and light chain. The antibody was stored at -80°C, suspended in PBS at a concentration of 3.36 mg/ml. Efficacy was tested using an in-house assay at Amgen Inc.

WT and TSLPR$^{-/-}$ mice received 1 mg of muM702 every 5 days, administered i.p., starting one day prior to tumor cell injection and continuing until the defined humane endpoints or day 60 was reached, whichever came first.

III. RESULTS

The purpose of this study was to test the hypothesis that TSLP promotes a permissive microenvironment for breast cancer, which facilitates the growth and metastasis of the primary tumor. We hypothesized that it does so, at least in part, by inducing the development of a Th2-mediated immune response, which likely leads to an ineffective anti-tumor response. To test this, we investigated the following parameters: (1) the immune response to 4T1-12B tumor cells both *in vitro* and *in vivo*; (2) the growth and metastasis of the primary tumor *in vivo*; (3) the effects of TSLP unresponsiveness in $TSLPR^{-/-}$ mice and in mice treated with a neutralizing anti-TSLP antibody *in vivo*; and, (4) the presence of TSLP in human tumors of the breast and/or normal glandular epithelium in the breast.

DECLARATION:

R. Erdmann performed all of the experiments in this study, with the exception of the experiments done using human breast tissue. Staff from the Manitoba Breast Tumor Bank prepared the TMA of normal and malignant breast tissue and optimized the conditions of the immunohistochemical assay used to stain the arrays for TSLP expression.

3.1. OBJECTIVE 1: CHARACTERIZE THE IMMUNE RESPONSE TO 4T1-12B TUMOR CELLS BOTH *IN VITRO* AND *IN VIVO*

3.1.1. 4T1-12B CELLS PRODUCE TSLP CONSTITUTIVELY *IN VITRO*

Figure 3 shows that, except for TSLP, each cytokine tested was below the level of detection. TSLP was present at mean concentration of 6643 pg/ml (n=3 cultures of 4T1-12B cells derived from different aliquots of frozen 4T1-12B cells.)

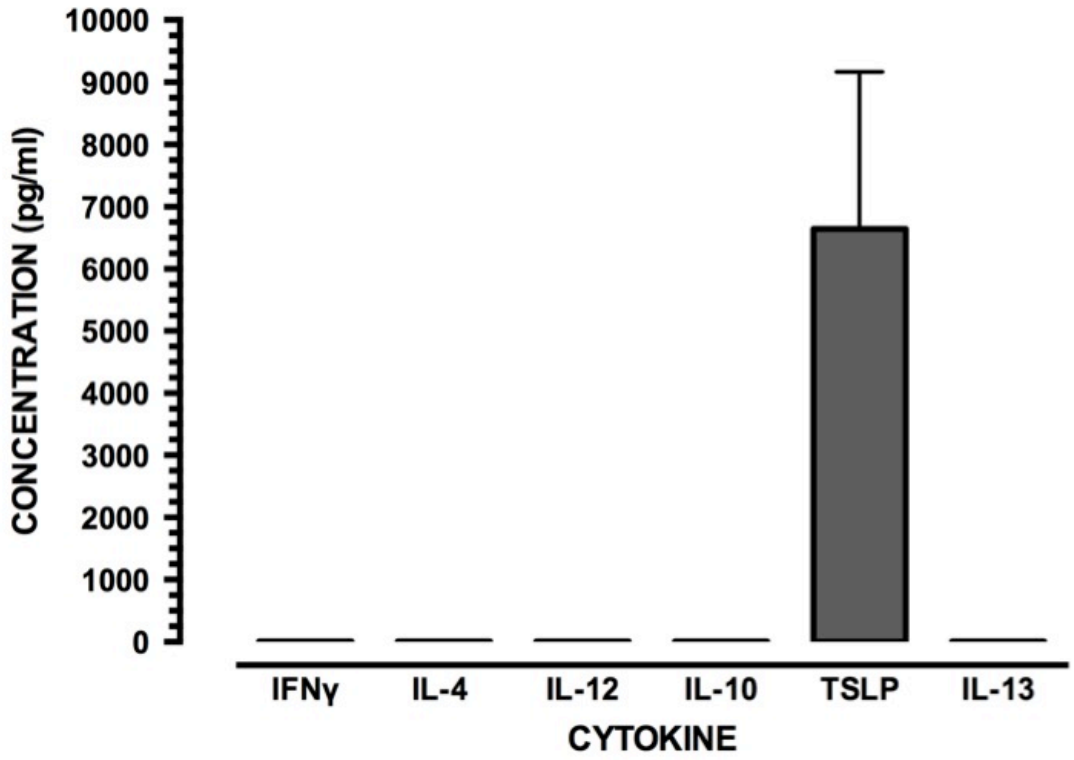

FIGURE 3. 4T1-12B CELLS PRODUCE TSLP CONSTITUTIVELY *IN VITRO*

One million unstimulated 4T1-12B cells were cultured in triplicate for 48 hours in complete RPMI media containing 5% FBS. Supernatants were tested for IFNγ, IL-4, IL-12(p40), IL-10, IL-13 and TSLP by ELISA. Bars represent the mean concentration of the indicated cytokine from three cultures from different 4T1-12B stock vials.

3.1.2. THE *DE NOVO* IMMUNE RESPONSE TO 4T1-12B TUMOR CELLS BY SPLENOCYTES FROM NAÏVE TSLPR$^{-/-}$ MICE IS SHIFTED TOWARDS TH1 CYTOKINE PRODUCTION

Figure 4 shows that IFNγ was present in significantly higher concentrations in cultures containing TSLPR$^{-/-}$ splenocytes, compared to WT splenocytes, when the splenocytes concentration was 10^7 cells/ml ($p<0.001$), 5 x 10^6 cells/ml ($p<0.001$), and 25 x 10^4 cells /ml ($p<0.01$). IL-4 was detectable in cultures containing splenocytes from WT mice at a splenocyte concentration of 10^7 cells/ml only (28 pg/ml compared to 0 pg/ml for the TSLPR$^{-/-}$ group, $p<0.05$). IL-4 was not detectable in any of the other cultures tested. The differences in IL-12, IL-10 and IL-13 concentrations were not significantly different in cultures of WT and TSLPR$^{-/-}$ splenocytes at any of the concentrations, with the exception of IL-13, when the concentration was significantly higher in the TSLPR$^{-/-}$ group at the lowest splenocytes concentration tested (23 pg/ml and 43 pg/ml, respectively; $p<0.05$). Overall, there was a trend towards decreasing concentrations of IFN-γ, IL-12, IL-10 and IL-13 over the course of the disease in the two experimental groups. The concentrations of TSLP in cultures containing splenocytes from either WT or TSLPR$^{-/-}$ mice were similar to those seen in cultures containing 4T1-12B alone ($p>0.05$ by ANOVA). Figure 4 shows data from one representative experiments that was performed three times with similar results. The mean concentrations of cytokines were compared in the two groups at each splenocyte concentration using a Student's t test.

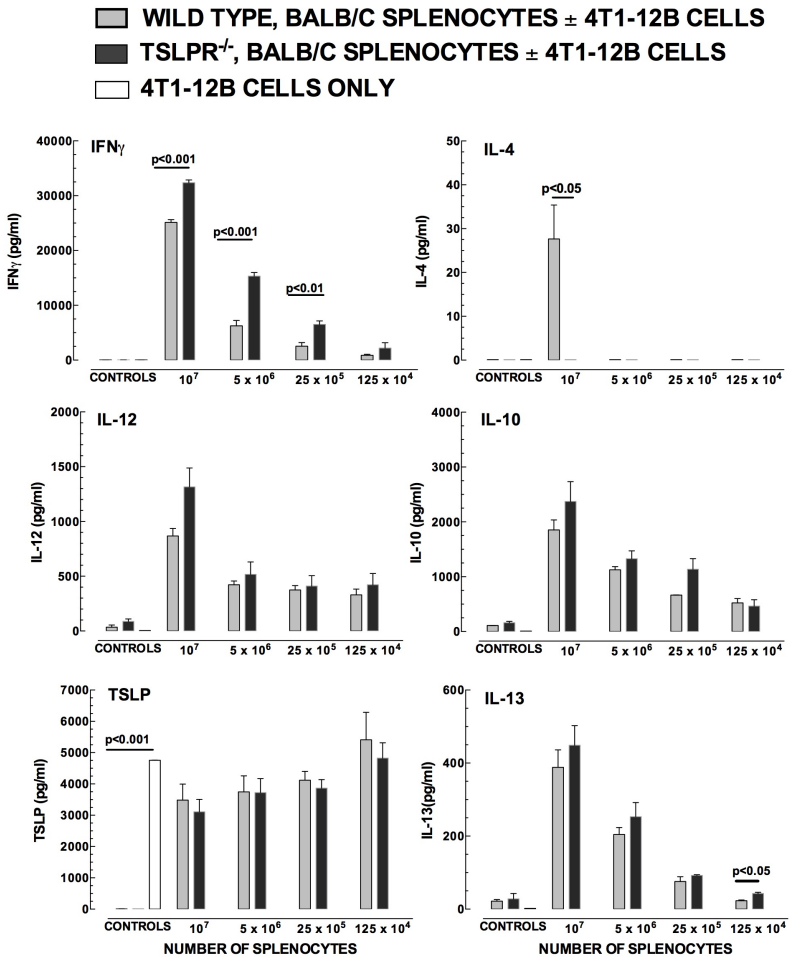

FIGURE 4. THE *DE NOVO* IMMUNE RESPONSE TO 4T1-12B TUMOR CELLS BY SPLENOCYTES FROM NAÏVE TSLPR$^{-/-}$ MICE IS SHIFTED TOWARDS TH1 CYTOKINE PRODUCTION

One hundred thousand 4T1-12B cells were cocultured with four concentrations of naïve, unstimulated splenocytes from WT or TSLPR$^{-/-}$ mice. Controls consisted of $1x10^7$ WT or TSLPR$^{-/-}$ splenocytes alone and $1x10^5$ 4T1-12B cells alone. Cultures were incubated for 48 hours and supernatants were assayed by ELISA to determine the concentration of IFNγ, IL-4, IL-10, IL-12(p40), IL-13 and TSLP. Differences in the mean concentrations of cytokines in the WT and TSLPR$^{-/-}$ groups were compared for each concentration of splenocytes, using a Student's t test.

3.1.3. SPLENOCYTES FROM NAÏVE WT AND TSLPR$^{-/-}$ MICE DO NOT EXHIBIT 4T1-12B-DIRECTED LYTIC ACTIVITY

Figure 5A shows that unstimulated splenocytes from naïve WT mice were able to lyse YAC-1 target cells with an efficiency of 2.6 lytic units but were unable to lyse 4T1-12B cells. Figure 5B shows that unstimulated splenocytes from TSLPR$^{-/-}$ mice were able to lyse YAC-1 cells with an efficiency of 3.2 lytic units but were also unable to lyse 4T1 cells. Figure 5 shows data one representative experiment that was performed three times with similar results.

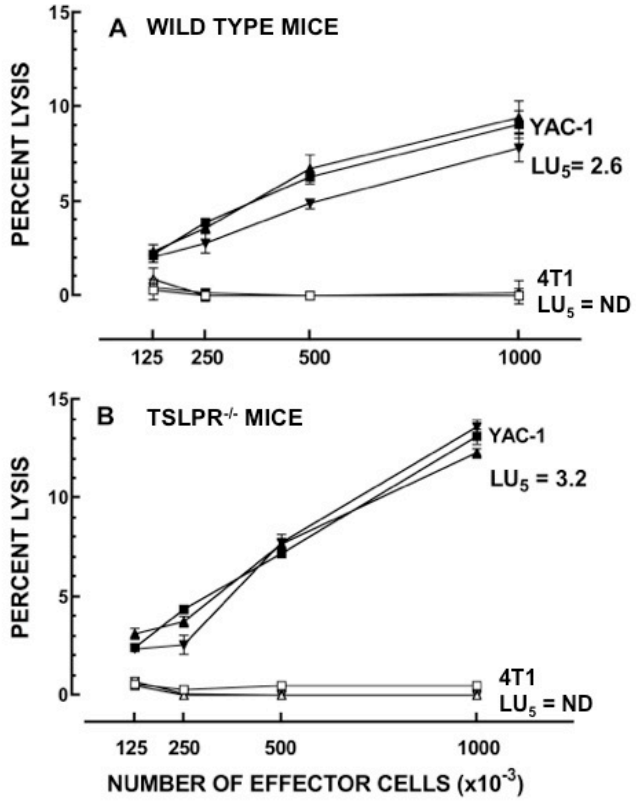

FIGURE 5. SPLENOCYTES FROM NAÏVE WT AND TSLPR$^{-/-}$ MICE DO NOT EXHIBIT 4T1-12B-DIRECTED LYTIC ACTIVITY

Cell-mediated cytotoxicity was measured in a 4-hour chromium-51 release assay. Unstimulated splenocytes from individual naïve WT (A) or TSLPR$^{-/-}$ (B) mice were incubated for 4 hours with ^{51}Cr-labeled 4T1-12B cells or positive control YAC-1 cells at the following effector to target ratios: 100:1, 50:1, 25:1 and 12.5:1. Lytic units (LU_5) were calculated using the exponential fit method, as described by Pross *et al.* [133] ND= not determined. n=3 mice/group/target. ■: YAC-1-directed lysis by WT effectors; □: 4T1-12B-directed lysis by WT effectors; ▲: YAC-1-directed lysis by TSLPR$^{-/-}$ effectors; △: 4T1-12B-directed lysis by TSLPR$^{-/-}$ effectors. Data shown is from one representative experiment that was performed three times with similar results.

3.2. Objective 2: Determine how the loss of TSLPR function affects the tumor establishment, growth and metastasis in the 4T1 mouse mammary tumor model

3.2.1. Primary tumors are established more often in WT mice than in $TSLPR^{-/-}$ mice

Table 1 shows that, of the 19 WT and 18 $TSLPR^{-/-}$ mice that were injected with $7x10^3$ 4T1-12B tumor cells, the number of mice in which primary tumors were successfully established was 18 and 11, respectively. Primary tumors were therefore established more often in WT mice compared to $TSLPR^{-/-}$ mice ($p<0.05$, Fisher's Exact test). Table 1 shows combined data from three separate experiments.

TABLE 1. PRIMARY TUMORS ARE ESTABLISHED MORE OFTEN IN WT MICE THAN IN TSLPR$^{-/-}$ MICE OVER A 60-DAY PERIOD

	Number of mice with a primary tumor[1]	Number of mice with no tumor[2]	Total	p-value
Wild-type	18	1	19	$p<0.05$[3]
TSLPR$^{-/-}$	11	7	18	
Total	29	8	37	

[1]The presence of a primary tumor was defined as a palpable mass of any size in the abdomen at any point post-injection (p.i.).

[2] The absence of a primary tumor was defined as no palpable mass of any size in the abdominal area at any time point p.i.

[3] The difference in the number of mice that either did or did not establish a primary tumor in the WT and TSLPR$^{-/-}$ groups were compared using a Fisher's Exact test. Data shown is from three separate experiments, combined.

3.2.2. PRIMARY TUMOR GROWTH IS SLOWER IN TSLPR$^{-/-}$ MICE

Figure 6 shows that the diameters of the primary tumors in the WT mice were significantly larger than those observed in TSLPR$^{-/-}$ mice at the following time points: day 27 (3.9 and 1.5 mm, respectively; $p<0.05$), day 30 (5.3 and 1.6 mm, respectively; $p<0.05$), day 35 (7.4 and 2.3 mm, respectively; $p<0.05$), day 38 (7.6 and 3.1 mm, respectively; $p<0.05$) and day 40 post-injection (7.9 and 3.4 mm, respectively; $p<0.05$). The mean tumor diameters in the two groups were compared at each time points using a Student's t test. Data shown is from two experiments, combined.

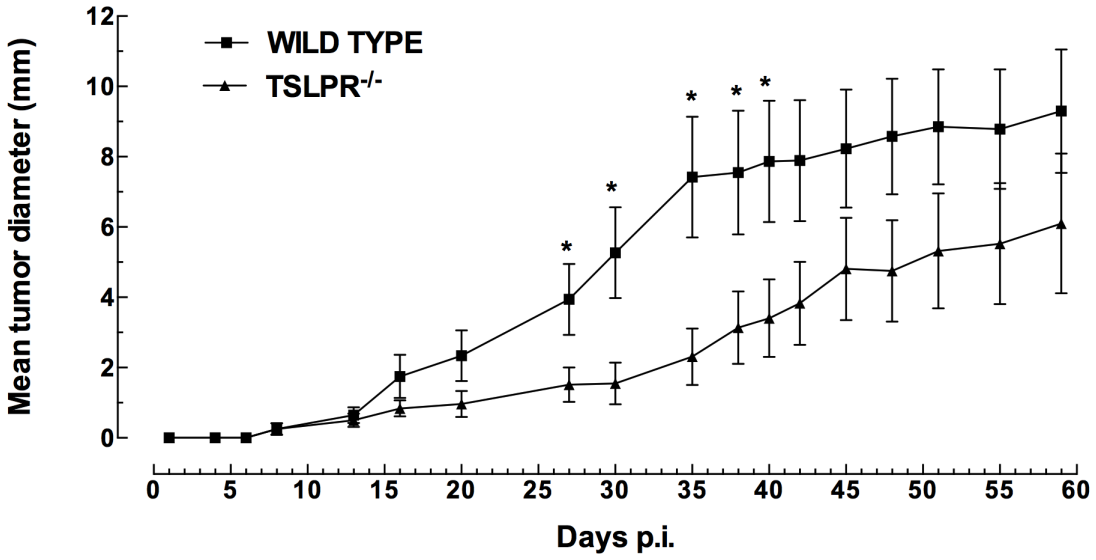

FIGURE 6. PRIMARY TUMOR GROWTH IS SLOWER IN TSLPR$^{-/-}$ MICE

Seven thousand 4T1-12B cells were injected into the mammary fat pad of 8-week old female WT or TSLPR$^{-/-}$ Balb/c mice (n=8/group/time-point). The diameter of the primary tumor was measured every 3-4 days p.i. with electronic digital vernier calipers. Mice were included if the primary tumor diameter increased beyond 1 mm and phantom diameters were retained in the calculation of the means if the mouse reached its humane end point prior to day 60. An asterisk indicates that the mean tumor diameters were significantly different in the two groups at that time point ($p<0.05$, Student's t test). n=8 mice/group/time point. Data shown is from two experiments, combined.

3.2.3. THE PATTERN OF 4T1-12B METASTASIS TO THE LUNGS OF WT AND TSLPR$^{-/-}$ MICE DIFFERS FROM THE PATTERN OF METASTASIS TO THE BRAIN OF WT AND TSLPR$^{-/-}$ MICE

Figure 7 shows the levels of metastasis to the lungs for mice that had reached their humane end point, determined by comparing the median number of photons/sec emitted from free luciferase in the organ lysate. The median number of photons/sec in WT mice was 55, whereas in TSLPR$^{-/-}$ mice, the median number was 9. This difference was found to be significant (55 photons/sec and 9 photons/sec, respectively; $p<0.05$ by Mann-Whitney test). Compared to TSLPR$^{-/-}$ mice, there was a greater range in the level of metastasis in lungs from WT mice, and a greater level of metastasis overall in this group. The signal emitted in lung tissue from WT mice ranged from 0 – 5372 photons/sec (n=15), while in TSLPR$^{-/-}$ lung tissue, the signal ranged from 0 – 33 photons/sec (n=6).

The results shown in Figure 8, which were also obtained from mice that had reached their humane end point, indicates that the median level of metastasis to the brain, was greater in TSLPR$^{-/-}$ mice compared to WT mice (31 photons/sec and 12 photons/sec, respectively, $p<0.05$ by Mann-Whitney test). The signals emitted from WT brain tissue ranged from 0 -28 photons/sec with an outlier of 126 photons/sec in one mouse, and a median of 12 photons/sec (n=13). In TSLPR$^{-/-}$ brain tissue, the signals emitted ranged from 29-48 photons/sec, with an outlier at 4 photons/sec and a median of 31 photons/sec (n=6).

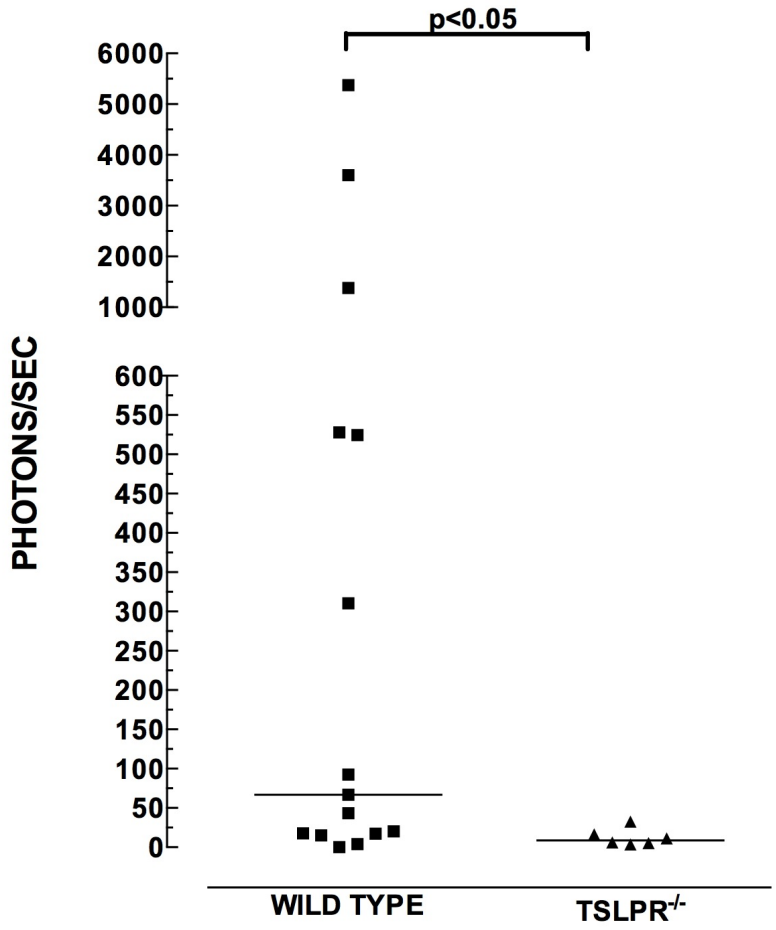

FIGURE 7. THE MEDIAN LEVEL OF METASTASIS TO THE LUNGS IS GREATER IN WT MICE, COMPARED TO TSLPR$^{-/-}$ MICE

Tumor-bearing mice that had reached their humane endpoint were euthanized and whole lungs were harvested and assayed for the presence of 4T1-12B cells by chemiluminescence, as described in the Materials and Methods. Symbols represent the number of photons/sec determined for whole lung lysates from an individual WT (■) or TSLPR$^{-/-}$ (▲) mouse. Medians, denoted by a horizontal line, were compared using a Mann-Whitney test. n(WT) = 15; n(TSLPR$^{-/-}$) = 6. Data is from three experiments, combined.

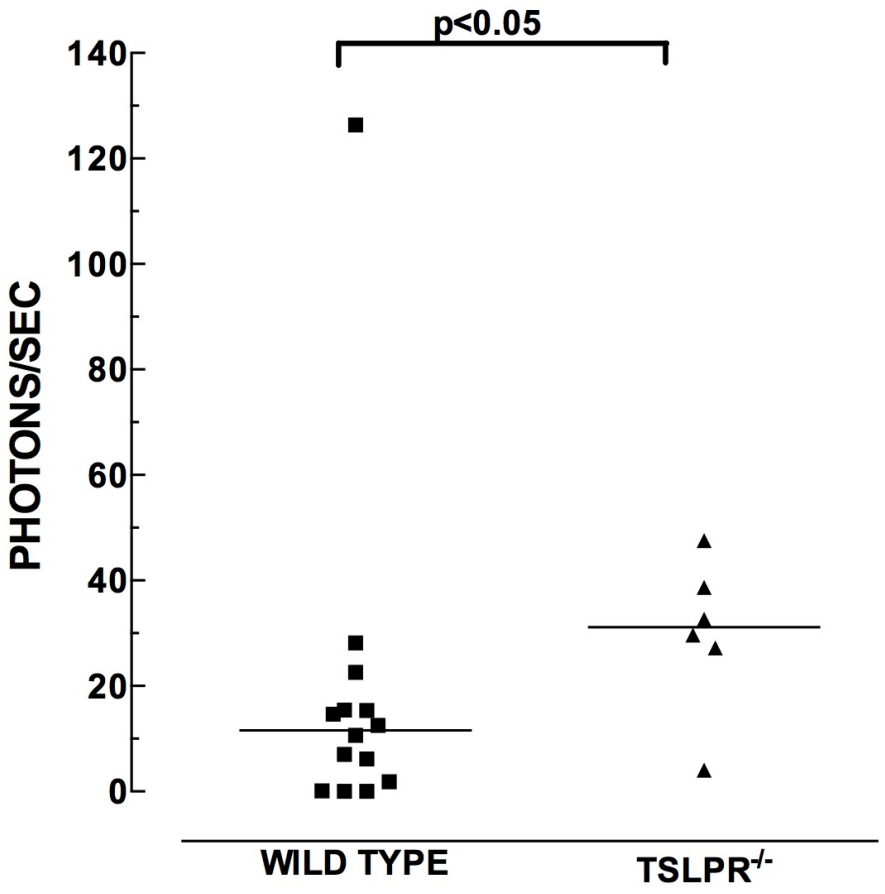

FIGURE 8. THE MEDIAN LEVEL OF METASTASIS TO THE BRAIN IS GREATER IN TSLPR$^{-/-}$ THAN IN WT MICE

Tumor-bearing mice that had reached their humane endpoint were euthanized and the whole brain was harvested and assayed for the presence of 4T1-12B cells by chemiluminescence, as described in the Materials and Methods. Symbols represent the number of photons/sec determined for whole lung lysates from an individual WT (■) or TSLPR$^{-/-}$ (▲) mouse. Medians were compared by Mann-Whitney test. n for WT = 14; n for TSLPR$^{-/-}$ = 6. Data shown is from three separate experiments, combined.

3.3. OBJECTIVE 3: DETERMINE HOW THE LOSS OF TSLPR FUNCTION AFFECTS THE CYTOKINE AND CYTOTOXICITY RESPONSES IN THE 4T1 MOUSE MAMMARY TUMOR MODEL

3.3.1. 4T1-12B-DIRECTED CYTOTOXICITY IS UNDETECTABLE IN BOTH WT AND TSLPR$^{-/-}$ MICE AFTER THE PRIMARY TUMOR HAS BEEN ESTABLISHED

Table 2 shows that, on days 7, 21 and 35 p.i., the level of 4T1-12B-directed cytotoxicity was undetectable in both WT or TSLPR$^{-/-}$ mice. In addition, the levels of YAC-1 directed cytotoxicity decreased in both WT and TSLPR$^{-/-}$ were lower than those seen in control mice at all time points tested.

TABLE 2. 4T1-12B – DIRECTED CYTOTOXICITY IS UNDETECTABLE IN BOTH WT AND TSLPR$^{-/-}$ MICE AFTER THE PRIMARY TUMOR HAS BEEN ESTABLISHED

	Wild-type mice (LU_5)[1]		**TSLPR$^{-/-}$ mice (LU_5)**	
	4T1-12B target cells	**YAC-1[4] target cells**	**4T1-12B target cells**	**YAC-1 target cells**
Control mice[2]	ND[3]	2.6 ± 0.3	ND	3.1 ± 0.1
Day 7 p.i.	ND	0.4 ± 0.2	ND	ND
Day 21 p.i.	ND	0.9 ± 0.9	ND	1.1 ± 0.6
Day 35 p.i.	ND	0.8 ± 0.7	ND	0.3 ± 0.3

[1] Lytic units were calculated according to the exponential fit described by Pross *et al.* [133]

[2] Age- and sex-matched WT or TSLPR$^{-/-}$ mice that had not been injected with tumor cells.

[3] ND: LU_5 not determined as percent lysis values were too low.

[4] Positive control cell line.

3.3.2. THE CYTOKINE PROFILE IN TUMOR-BEARING TSLPR$^{-/-}$ MICE IS SHIFTED AWAY FROM TH2-DOMINATED IMMUNITY AND TOWARDS TH1-DOMINATED IMMUNITY OVER A 60-DAY PERIOD

Figure 9 shows that concentrations of IFNγ were significantly higher ($p<0.05$ by Student's t test) in splenocytes cultures from TSLPR$^{-/-}$ mice on days 21, 28 and 60 (831 pg/ml, 512 pg/ml, and 150 pg/ml, respectively), compared to those seen in cultures from WT mice (434 pg/ml, 232 pg/ml, 19 pg/ml; $p<0.05$). IL-4 reached higher levels in splenocyte cultures from WT mice compared to TSLPR$^{-/-}$ mice at each time point tested; however, this difference was only significant on day 7 (115 pg/ml and 44 pg/ml, respectively; $p<0.05$) when the concentration was higher in WT mice. Neither IL-12(p40) or IL-13 showed a discernible pattern of cytokine concentrations in cultures from WT or TSLPR$^{-/-}$ at any time point. However, IL-13 was significantly higher in TSLPR$^{-/-}$ cultures than in WT cultures on day 21 (568 pg/ml and 767 pg/ml, respectively; $p<0.05$). IL-10 levels were not significantly different in WT and TSLPR$^{-/-}$ cultures. TSLP was undetectable until day 21, when it was found in supernatant from WT splenocytes but not in TSLPR$^{-/-}$ cultures (19 pg/ml and 2 pg/ml, respectively; $p<0.001$). TSLP was present in both WT and TSLPR$^{-/-}$ supernatants on day 60 only. The concentrations of IFNγ, IL-4 and IL-10 declined steadily in both WT and TSLPR$^{-/-}$ mice after day 14 post-injection.

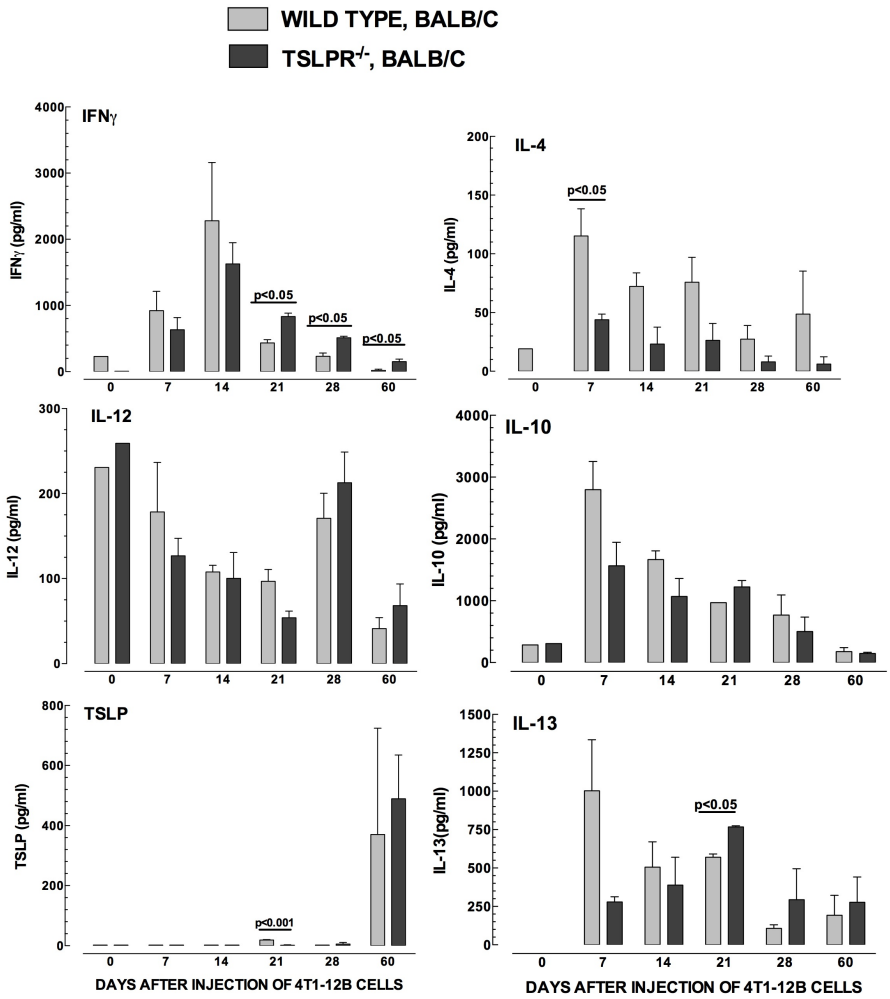

FIGURE 9. THE CYTOKINE PROFILE IN TUMOR-BEARING TSLPR$^{-/-}$ MICE IS SHIFTED AWAY FROM TH2-DOMINATED IMMUNITY AND TOWARDS TH1-DOMINATED IMMUNITY OVER A 60-DAY PERIOD

Seven thousand 4T1-12B cells were injected into the mammary fat pad of 8-week female WT or TSLPR$^{-/-}$ mice. Spleens were harvested every 7 days p.i. until day 28, and then again on day 60 p.i. Splenocytes were cultured for 48 hours. ELISA was used to measure the following cytokines in the supernatants: IFNγ, IL-4, IL-10, IL-12(p40), IL-13 and TSLP. Differences in the mean concentrations of cytokines were compared in the

WT and TSLPR$^{-/-}$ groups, at each time point, using a Student's t test (n=3/group/time-point). Data shown is from one representative experiment performed twice.

3.3.3. PRIMARY TUMORS PRODUCE TSLP *EX VIVO*

Figure 10 shows that the concentrations of IFNγ, IL-4, IL-10 and IL-13 were below the level of detection in supernatants from cultures of dissociated primary tumors from WT and TSLPR$^{-/-}$ mice that had reached their humane endpoint (mean day 55). The concentration of IL-12(p40) was significantly higher in primary tumor cell cultures obtained from the TSLPR$^{-/-}$ group than in the WT group (149 pg/ml and 27 pg/ml, respectively; $p<0.05$ by Student's t test). TSLP was present in supernatants from both groups of mice; however, the mean concentrations did not differ significantly (n=3 /group.

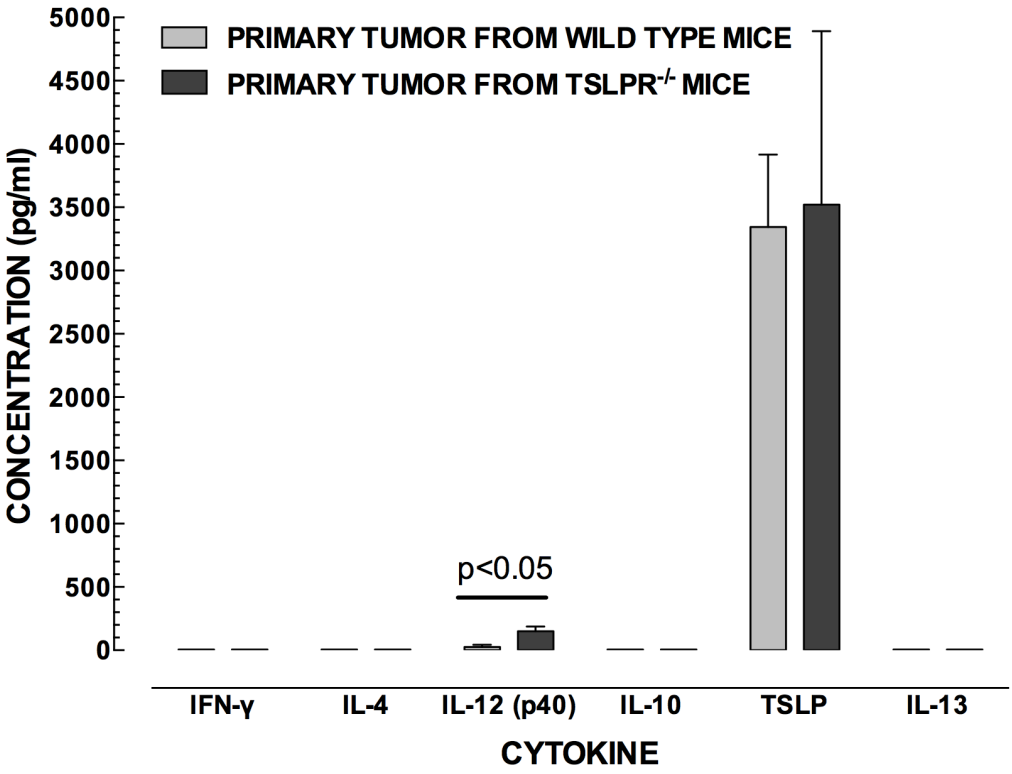

FIGURE 10. PRIMARY TUMORS PRODUCE TSLP *EX VIVO*

Primary tumors were dissected from WT or TSLPR$^{-/-}$ mice at their humane endpoint (mean day 55) and dissociated under sterile conditions. Supernatants were collected after 48 hours from cultures containing $2x10^6$ live cells . ELISA was used to measure the following cytokines in the supernatants: IFNγ, IL-4, IL-10, IL-12(p40), IL-13 and TSLP. Differences in the mean concentrations of cytokines were compared in the WT and TSLPR$^{-/-}$ groups, at each time point, using a Student's t test (n=3/group/time-point).

3.4. OBJECTIVE 4: DETERMINE WHETHER TREATMENT WITH AN ANTI-TSLP NEUTRALIZING ANTIBODY AFFECTS THE ESTABLISHMENT, GROWTH AND METASTASIS OF THE PRIMARY TUMOR IN THE 4T1 MOUSE MAMMARY TUMOR MODEL

As an alternative approach to using TSLPR$^{-/-}$ mice to study the role of TSLP in the 4T1 mouse mammary tumor model, we obtained an anti-TSLP mAb, known as muM702, from Amgen, Inc. This antibody had been used in other in mouse models of disease [123] and Amgen had confirmed its ability to neutralize TSLP (see Materials & Methods on page 30). We were primarily interested in examining the effect of muM702 treatment on WT mice, but included a group in which TSLPR$^{-/-}$ mice were also treated with muM702 to determine whether some of the differences we had observed when we compared WT and TSLPR$^{-/-}$ mice could be further increased by the addition of muM702 treatment *in vivo*.

3.4.1. TREATMENT WITH THE ANTI-TSLP NEUTRALIZING ANTIBODY, MUM702, DOES NOT INHIBIT THE ESTABLISHMENT OF PRIMARY TUMORS IN WT OR TSLPR$^{-/-}$ MICE

Table 3 shows that there was no significant difference in the number of untreated (5/6) and antibody-treated (6/6) WT mice that developed primary tumors ($p>0.05$, Fisher's Exact test). Table 4 shows that the number of untreated TSLPR$^{-/-}$ mice that developed tumors (2/6) was higher than the number of antibody-treated (5/6) TSLPR$^{-/-}$ mice that developed primary tumors, but this difference was not statistically significant ($p>0.05$, Fisher's Exact test). Data shown is from a single pilot experiment.

TABLE 3. TREATMENT WITH THE ANTI-TSLP NEUTRALIZING ANTIBODY, MUM702, DOES NOT INHIBIT THE ESTABLISHMENT OF PRIMARY TUMORS IN WT MICE

	Number of mice with a primary tumor[1]	Number of mice with no primary tumor[2]	Total	p value[4]
WT (Untreated)	5	1	6	n.s.
WT (muM702)[3]	6	0	6	p>0.05
Total	11	1	12	

[1] The presence of a primary tumor was defined as a palpable mass of any size in the abdomen at any point post-injection (p.i.).

[2] The absence of a primary tumor was defined as no palpable mass of any size in the abdominal area at any time point p.i.

[3] One milligram of muM702 mouse anti-mouse TSLP neutralizing antibody was administered to mice one day prior to 4T1-12B cell injection and then every five days until day 60 or until the humane endpoint was reached.

[4] The numbers of mice in each of the two groups that either did or did not establish a primary tumor were compared using Fisher's exact test.

TABLE 4. TREATMENT WITH THE ANTI-TSLP NEUTRALIZING ANTIBODY, MUM702, DOES NOT INHIBIT THE ESTABLISHMENT OF PRIMARY TUMORS IN $TSLPR^{-/-}$ MICE

	Number of mice with a primary tumor[1]	Number of mice with no primary tumor[2]	Total	p-value[4]
$TSLPR^{-/-}$ (Untreated)	2	4	6	n.s.
$TSLPR^{-/-}$ (muM702)[3]	5	1	6	p>0.05
Total	7	5	12	

[1] The presence of a primary tumor was defined as a palpable mass of any size in the abdomen at any point post-injection (p.i.).

[2] The absence of a primary tumor was defined as no palpable mass of any size in the abdominal area at any time point p.i.

[3] One milligram of muM702 mouse anti-mouse TSLP neutralizing antibody was administered to mice one day prior to 4T1-12B cell injection and then every five days until day 60 or until the humane endpoint was reached.

[4] The numbers of mice in each of the two groups that either did or did not establish a primary tumor were compared using Fisher's exact test.

3.4.2. TREATMENT WITH THE ANTI-TSLP NEUTRALIZING ANTIBODY, MUM702, DOES NOT INHIBIT THE GROWTH OF THE PRIMARY TUMOR IN WT OR TSLPR$^{-/-}$ MICE

Figure 11 shows that the differences in the sizes of the primary tumors in the antibody-treated treated mice were not significantly different from those seen in the corresponding untreated control mice at any of the time points tested (Student's t test, $p>0.05$ for all time points tested). This was true for both the WT (Figure 11A) and TSLPR$^{-/-}$ groups (Figure 11B). Although not significant, it appears that antibody treatment might enhance the growth of the primary tumor in both WT and TSLPR$^{-/-}$ mice. Figure 11 shows results from one experiment.

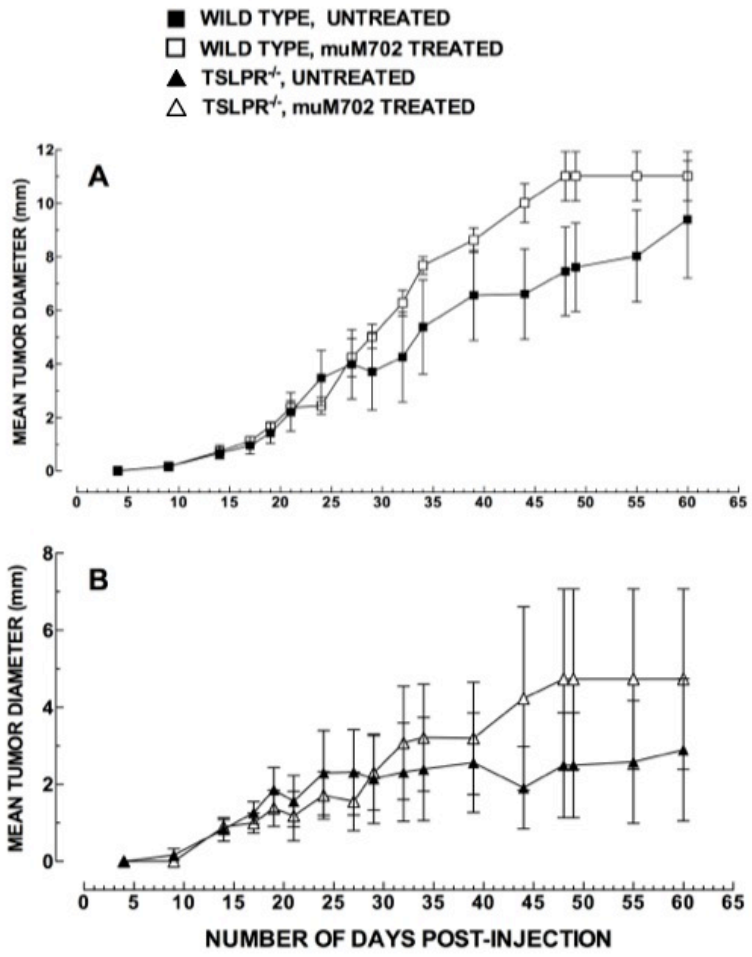

FIGURE 11. TREATMENT WITH THE ANTI-TSLP NEUTRALIZING ANTIBODY, MUM702, DOES NOT INHIBIT GROWTH OF THE PRIMARY TUMOR IN WT OR TSLPR$^{-/-}$ MICE

WT (A) and TSLPR$^{-/-}$ (B) mice were treated with 1 mg of the anti-TSLP neutralizing antibody, muM702, i.p., one day prior to the injection of 4T1-12B cells. The antibody was then injected once every 5 days until the mice reached their humane endpoint or until day 60, which ever came first. Differences in the mean tumor diameters were compared in the WT groups and the TSLPR$^{-/-}$ groups at each time point using a Student's t test. No significant differences were observed ($p>0.05$ for all time-points). n=6/group/time point. Data shown is from one pilot experiment.

3.4.3. NEUTRALIZING TSLP INHIBITS METASTASIS TO THE LUNGS OF WT MICE BUT DOES NOT AFFECT METASTASIS TO THE BRAIN OF WT OR TSLPR$^{-/-}$ MICE

Figure 12A shows the extent of metastasis to the lungs of untreated and muM702-treated WT mice that had reached their humane end point (mean day 55). The median signal emitted in the lungs was significantly higher in untreated WT mice than in WT mice treated with muM702 (55 photons/sec and 15 photons/sec, respectively; $p<0.05$, Mann-Whitney test). Figure 12B shows metastasis to the lungs of untreated and muM702-treated TSLPR$^{-/-}$ mice. Although muM702-treated TSLPR$^{-/-}$ mice appeared to have more metastatic cells in their lungs, the difference was not found to be significant ($p>0.05$; Mann-Whitney test).

Figure 13A shows that the extent of metastasis to the brain of muM702-treated and untreated WT mice that had reached their humane endpoint (mean day 55) were not significantly different ($p>0.05$, Mann-Whitney test). Similarly, Figure 13B shows metastasis to the brain of muM702-treated and untreated TSLPR$^{-/-}$ mice that had reached their humane endpoint were not significantly different. ($p>0.05$; Mann-Whitney test).

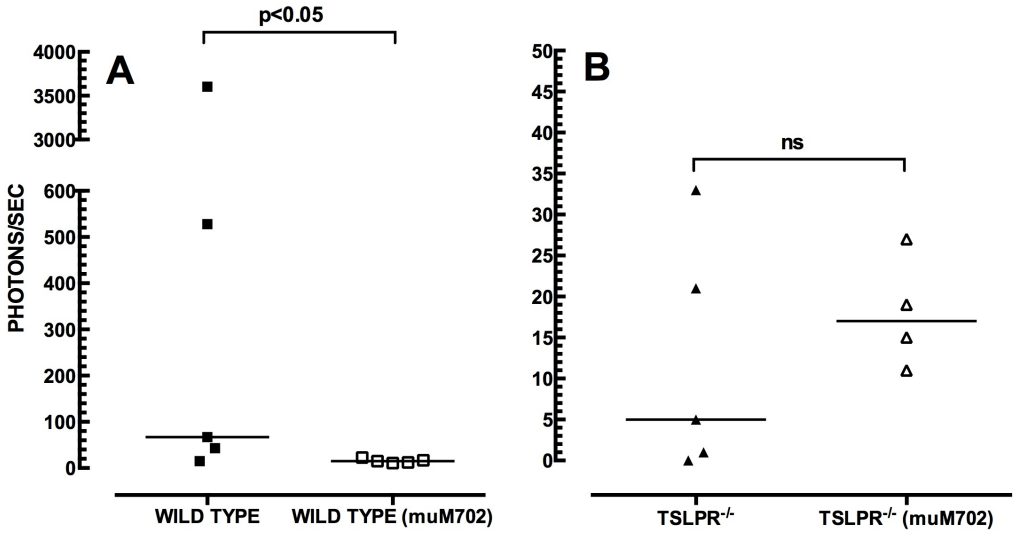

FIGURE 12. NEUTRALIZING TSLP SIGNIFICANTLY REDUCES METASTASIS TO THE LUNGS OF TUMOR-BEARING WT MICE BUT DOES NOT SIGNIFICANTLY AFFECT LUNG METASTASIS IN TUMOR-BEARING TSLPR$^{-/-}$ MICE

Tumor-bearing WT (A) or TSLPR$^{-/-}$ (B) mice, either treated with muM702 antibody or left untreated, were euthanized at their humane endpoints (mean day 55 p.i.). Whole lungs were harvested and assayed for the presence of 4T1-12B cells by chemiluminescence, as described in the Materials and Methods. Symbols represent the number of photons/second determined for whole lung lysates from an individual mouse, according to this legend: ■: WT untreated, n=6; □: WT muM702-treated, n=5; ▲: TSLPR$^{-/-}$ untreated, n=5; △: TSLPR$^{-/-}$ muM702-treated, n=4. A horizontal line denotes the median for each group. Differences in the medians between corresponding experimental groups were compared using a Mann-Whitney test. Data shown is from one pilot experiment.

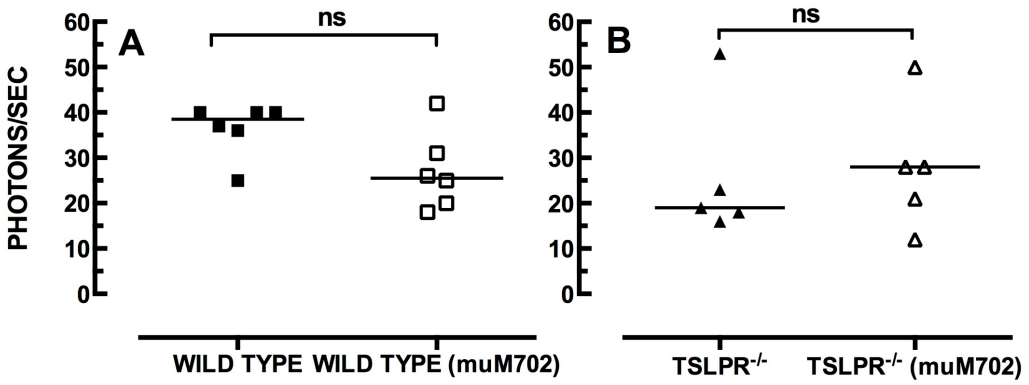

FIGURE 13. NEUTRALIZING TSLP DOES NOT AFFECT METASTASIS TO THE BRAIN OF TUMOR-BEARING WT OR TSLPR$^{-/-}$ MICE

Tumor-bearing WT (A) or TSLPR$^{-/-}$(B) mice, either treated with muM702 antibody or left untreated, were euthanized at their humane endpoints (mean day 55 p.i.). Whole brains were harvested and assayed for the presence of 4T1-12B cells by chemiluminescence, as described in the Materials and Methods. Symbols represent the number of photons/second determined for whole brain lysates from an individual mouse, according to this legend: ■: WT untreated, n=6; □: WT muM702-treated, n=5; ▲: TSLPR$^{-/-}$ untreated, n=5; △: TSLPR$^{-/-}$ muM702-treated, n=4. A horizontal line denotes the median for each group. Differences in the medians in corresponding experimental groups were compared using a Mann-Whitney test. Data shown is from one pilot experiment.

3.5. Objective 5: To examine TSLP expression in human invasive breast cancer and normal tissue using tissue microarray analysis

3.5.1. TSLP is expressed in normal breast tissue and in human invasive breast cancer

Figure 14 shows that glandular epithelium from normal tissue stained positively for TSLP. Tumor tissue also stained positively for TSLP, with the most intense staining located within the tumor cells and some less intense staining present in foci within the stroma.

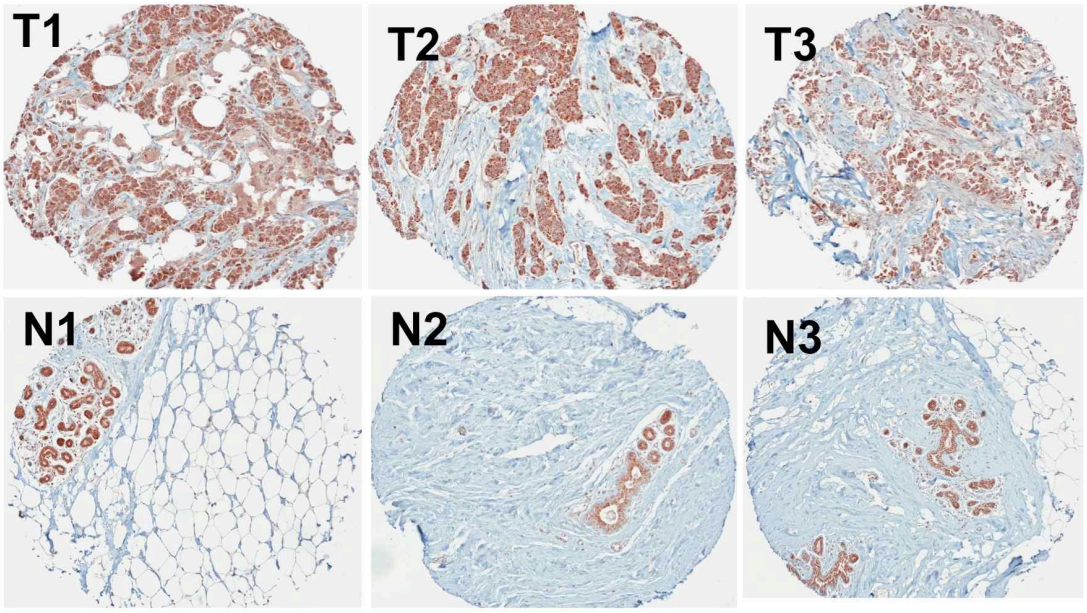

FIGURE 14. TSLP IS EXPRESSED IN NORMAL BREAST TISSUE AND IN HUMAN INVASIVE BREAST CANCER

Tissue microarrays (TMA) were prepared from formalin-fixed, paraffin-embedded tissue from the Manitoba Breast Tumor Bank. TSLP expression (staining brown) is present in both breast tumors (T) and normal breast tissue (N) that had been procured from mammoplasty reduction surgery. Representative cores from three different patients (T1, T2 and T3) are shown, along with representative cores of normal breast tissue from three individuals (N1, N2 and N3). Fifty cores were examined in each group. Sections were stained immunohistochemically with rabbit anti-human TSLP polyclonal antibody at a dilution of 1:100.

3.6. ADDITIONAL FINDINGS FROM AN EXPERIMENT IN WHICH MICE WERE MAINTAINED IN A NEWLY ACQUIRED, INDIVIDUALLY VENTILATED CAGING (IVC) SYSTEM

Near the end of our study, Central Animal Care Services implemented a change in the way animals are housed in their facility. Instead of being housed in conventional cages open to the air, mice were housed in individually ventilated cages (IVC), receiving HEPA filtered air.

3.6.1. THE NUMBERS OF WT OR TSLPR$^{-/-}$ MICE THAT ESTABLISHED A PRIMARY TUMOR WAS NOT SIGNIFICANTLY DIFFERENT WHEN EITHER CONVENTIONAL HOUSING OR IVC HOUSING WAS USED.

Table 5 shows the number of WT mice that developed tumors in IVC (7/8) and conventional housing (8/9). The difference was not significant ($p>0.05$, Fisher's Exact test). Table 6 shows the number of TSLPR$^{-/-}$ mice that developed tumors in IVC (7/8) and conventional housing (5/9). Although it appears that primary tumors were established less readily in TSLPR$^{-/-}$ mice housed conventionally, the difference did not achieve statistical significance ($p>0.05$; Fisher's Exact test).

TABLE 5. THE EFFECT OF IVC HOUSING ON PRIMARY TUMOR ESTABLISHMENT IN WT MICE

	Number of mice with a primary tumor[1]	Number of mice with no tumor[2]	Total	p-value[5]
WT (IVC[3])	7	1	8	n.s.
WT (CH[4])	8	1	9	p>0.05
Total	15	2	17	

[1] The presence of a primary tumor was defined as a palpable mass of any size in the abdomen at any point post-injection (p.i.).

[2] The absence of a primary tumor was defined as no palpable mass of any size in the abdominal area at any time point p.i.

[3] IVC: individually ventilated cages

[4] CH: conventional housing

[5] The numbers of mice in each of the two groups that either did or did not establish a primary tumor were compared using Fisher's exact test.

TABLE 6. THE EFFECT OF IVC HOUSING ON PRIMARY TUMOR ESTABLISHMENT IN TSLPR$^{-/-}$ MICE

	Number of mice with a primary tumor[1]	Number of mice with no tumor[2]	Total	p-value[5]
TSLPR$^{-/-}$ (IVC)	7	1	8	n.s.
TSLPR$^{-/-}$ (CH)	5	4	9	p>0.05
Total	12	5	17	

[1] The presence of a primary tumor was defined as a palpable mass of any size in the abdomen at any point post-injection (p.i.).

[2] The absence of a primary tumor was defined as no palpable mass of any size in the abdominal area at any time point p.i.

[3] IVC: individually ventilated cages

[4] CH.: conventional housing

[5]The numbers of mice in each of the two groups that either did or did not establish a primary tumor were compared using Fisher's exact test.

3.6.2. IVC HOUSING INHIBITS GROWTH OF THE PRIMARY TUMOR IN WT MICE BUT NOT IN TSLPR$^{-/-}$ MICE

Figure 15 shows that, when primary tumor growth was compared in mice housed in the two environments, the mean tumor diameters on day 35 for WT mice housed in IVC was smaller compared to WT mice housed in regular cages (7.4 mm and 3.7 mm, respectively; $p<0.05$). After day 35, WT tumors in conventional housing were larger than WT tumors in IVC housing, but the differences were not significant. There were no significant differences in the diameters of the primary tumors in TSLPR$^{-/-}$ mice housed in the two environments at any time point tested.

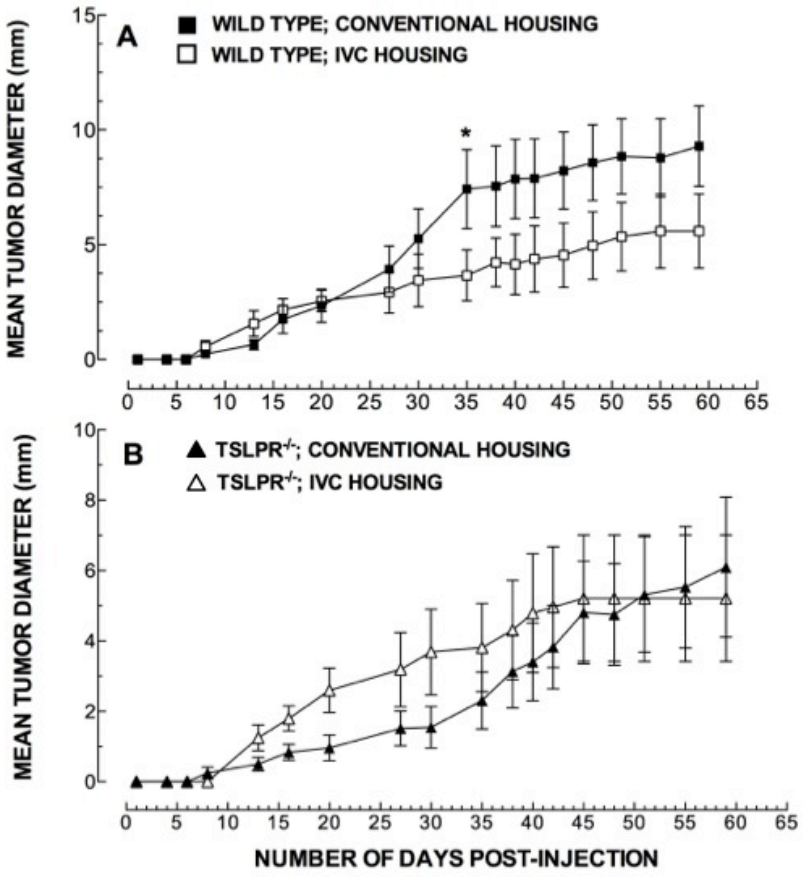

FIGURE 15. IVC HOUSING INHIBITS GROWTH OF THE PRIMARY TUMOR IN WT MICE BUT NOT IN TSLPR$^{-/-}$ MICE

WT (A) or TSLPR$^{-/-}$ (B) mice in IVC housing received 7x10^3 4T1-12B cells injected s.c. into the mammary fat pad. The diameters of the primary tumors were measured every 3-4 days until day 60 p.i. n=6/group/time-point. Differences in the mean tumor diameters were compared in the WT and TSLPR$^{-/-}$ mice at each time point using a Student's t test. Primary tumors in WT mice housed in conventional cages were significantly larger at day 35 p.i. than their IVC-housed counterparts ($p<0.05$, Student's t test). Data shown in the Figure is from one experiment performed in each housing condition.

3.6.3. IFNγ, IL-4 AND IL-10 CONCENTRATIONS ARE SIGNIFICANTLY LOWER IN BOTH WT AND TSLPR$^{-/-}$ MICE IN IVC HOUSING, COMPARED TO THOSE IN CONVENTIONAL HOUSING

Figure 16A shows the difference between concentrations of IFNγ, IL-4 and IL-10 in supernatants from WT mice in IVC and conventional housing. At all time points (day 7,14,21 and 28 p.i.), IFNγ concentrations were significantly higher in mice in conventional cages (923 pg/ml, 2280 pg/ml, 434 pg/ml and 232 pg/ml, respectively) than from mice in IVC housing (22 pg/ml, 28 pg/ml, 124 pg/ml and 11 pg/ml, respectively; $p<0.05$ by Student's t test). On days 7, 14 and 21, the concentrations of IL-4 (115 pg/ml, 72 pg/ml, and 76 pg/ml, respectively) and IL-10 (2797 pg/ml, 1667 pg/ml and 970 pg/ml, respectively) from WT mice in conventional housing were significantly higher than their IVC-housed counterparts (IL-4: 0.5 pg/ml, 1 pg/ml and 2 pg/ml, respectively; IL-10: 101 pg/ml, 107 pg/ml, and 163 pg/ml, respectively. Student's t test, $p<0.01$). For both IL-4 and IL-10, the differences in cytokine concentration on day 28 were not significantly different ($p>0.05$ by Student's t test).

Figure 16B shows the difference between concentrations of IFNγ, IL-4 and IL-10 in supernatants from TSLPR$^{-/-}$ mice in IVC and conventional housing. Similar to the results in WT mice, IFNγ was higher at all four time points (day 7, 14, 21 and 28 p.i.) in mice in conventional cages (634 pg/ml, 1608 pg/ml, 831 pg/ml and 512 pg/ml, respectively) than in mice in IVC housing (22 pg/ml, 29 pg/ml, 66 pg/ml and 11 pg/ml, respectively; $p<0.05$ by Student's t test). IL-4 was significantly higher in TSLPR$^{-/-}$ mice housed in conventional cages on day 7 (44 pg/ml and 0 pg/ml, respectively; $p<0.005$ by Student's t test). For all other time points, the differences were not significant ($p>0.05$ by

Student's t test) IL-10 followed the same pattern of significance as the WT mice. On days 7, 14 and 21, the cytokine concentration in mice from conventional cages (2307 pg/ml, 1070 pg/ml and 1225 pg/ml, respectively) was significantly higher than in mice from IVC housing (64 pg/ml, 83 pg/ml and 201 pg/ml, respectively; $p<0.05$ by Student's t test). Differences on day 28 were not significant ($p>0.05$; Student's t test).

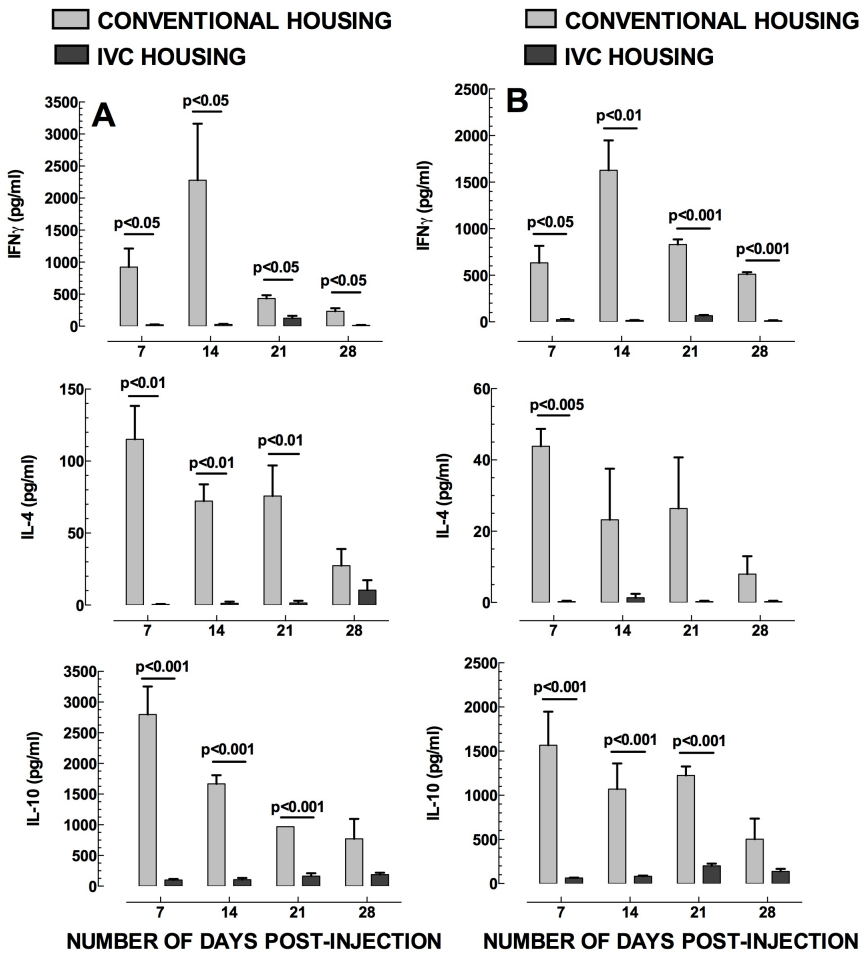

FIGURE 16. IFNγ, IL-4 AND IL-10 CONCENTRATIONS ARE SIGNIFICANTLY LOWER IN BOTH WT AND TSLPR$^{-/-}$ MICE IN IVC HOUSING, COMPARED TO THOSE IN CONVENTIONAL HOUSING

Seven thousand 4T1-12B cells were injected into the mammary fat pad of 8-week female WT (A) or TSLPR$^{-/-}$ (B) mice as described in the materials and methods. Mice were maintained in either IVC or conventional housing. Spleens were harvested every 7 days p.i. until day 28. Splenocytes were cultured for 48 hours and supernatant was collected and ELISA was used to measure IFNγ, IL-4, and IL-10. Differences in the mean concentrations of cytokines present at each time point in WT mice housed in IVC housing and conventional housing were compared using a Student's t test. Similar comparisons were made for TSLPR$^{-/-}$ mice housed in the two conditions. n=3 mice/time point/group.

3.6.4. TSLP PRODUCTION BY 4T1-12B CELLS IS NOT AFFECTED BY IVC HOUSING

Figure 17 shows that there were no significant differences in the concentrations of TSLP in supernatants from cultures of dissociated primary tumors that were harvested from WT (Figure 17A) housed in IVC conditions or conventional housing conditions (Student's t test, $p>0.05$). The same was true for primary tumors from $TSLPR^{-/-}$ (Figure 17B) mice housed in the two conditions ($p>0.05$). Tumors were harvested from mice that had reached their humane endpoints (mean day 55).

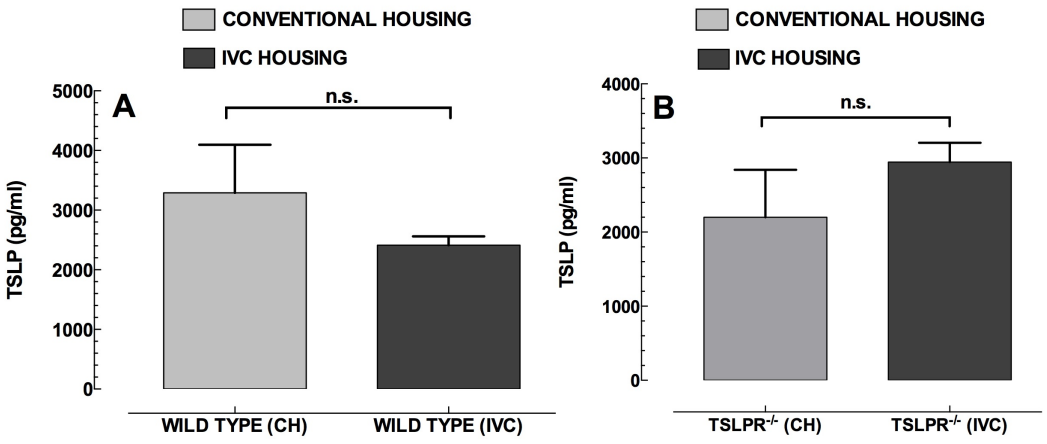

FIGURE 17. IVC HOUSING DOES NOT AFFECT THE CONCENTRATION OF TSLP IN CULTURES OF PRIMARY TUMOR CELLS RECOVERED FROM WT OR TSLPR$^{-/-}$ MICE

Primary tumors were recovered from WT (A) or TSLPR$^{-/-}$ (B) mice euthanized at their humane endpoint (mean day 55) and dissociated under sterile conditions. Supernatant were collected from cultures of $2x10^6$ live cells after 48 hours. ELISA was used to measure the concentration of TSLP in the supernatant samples (n=3). Differences in the mean concentrations of TSLP for the two types of housing conditons were compared for WT and TSLP using Student's t tests. No significant differences were observed amongst the groups ($p>0.05$ for all comparisons.)

IV. DISCUSSION

The central hypothesis for this study was that TSLP promotes a permissive microenvironment for breast cancer, which facilitates the growth and metastasis of the primary tumor. We further postulated that it does so, at least in part, by inducing the development of a Th2-mediated immune response, which likely leads to an ineffective anti-tumor response.

The rationale for our hypothesis was based first on an earlier observation made by our research team that 4T1-12B mouse mammary carcinoma cells line constitutively produce TSLP *in vitro* and, secondly, on our knowledge that TSLP derived from epithelia plays an important role in shaping developing immune responses in other conditions, such as allergy and asthma [116, 117]. The 4T1 model of breast cancer that we used for our study closely mimics the metastatic, basal-like, triple negative breast cancer subtype seen in humans[15-17]. Our primary experimental approach involved comparing several parameters of the disease in wild type mice and mice that lack the TSLP receptor. We found that, in the absence of TSLP responsiveness, primary tumors were established less often (Table 1); the diameters of the primary tumors were smaller during early tumor development (Fig. 6); the immune response was shifted away from Th2 immunity (Fig. 9); and, although the level of metastasis to the lung was reduced, the level of the metastasis to the brain was increased (Fig. 7 and 8). We also performed a pilot experiment in which we investigated the effects of an anti-TSLP neutralizing antibody on the establishment (Tables 3 and 4) and growth of the primary tumor (Fig. 11), as well as levels of metastasis to the lung and brain in WT and TSLPR$^{-/-}$ mice (Fig. 12 and 13). The only significant effect that we observed was that metastasis to the lung was significantly

reduced in WT mice treated that had been treated with the antibody. Interestingly, an examination of human breast cancer tissue and normal human breast tissue showed that both tumor cells and normal glandular epithelial stained positively for TSLP.

Since our research team had made the observation that 4T1-12B tumor cells secrete TSLP constitutively, (Fig. 3) another group has made a similar observation [44]. To begin to elucidate how TSLP might be shape the anti-tumor immune response, we first compared cytokine and cytotoxicity responses when splenocytes from naïve WT and naïve TSLPR$^{-/-}$ mice are exposed to 4T1-12B cells for the first time. We found that the cytokine profile was shifted away from a Th2-dominated immune response and towards a Th1-dominated immune response (Fig. 4) when splenocytes from TSLPR$^{-/-}$ were used, a finding that demonstrates that TSLP can regulate the innate *de novo* cytokine responses to 4T1-12B cells. When we compared the ability of naïve splenocytes from WT or TSLPR$^{-/-}$ mice to spontaneously lyse 4T1-12B cells no detectable lysis was observed in either group (Fig. 5). This finding was not entirely surprising, since it had previously been reported that 4T1 cells are poorly immunogenic[45]. As a positive control, we compared the ability of splenocytes from the two groups to lyse the definitive NK target cell line, YAC-1 (H-2$^{k/d}$). Both WT and TSLPR$^{-/-}$ splenocytes were able to lyse YAC-1 target cells effectively, indicating that NK cells with cytotoxic function were present in both groups. This finding shows that the absence of TSLP responsiveness does not affect the ability of naïve splenocytes to spontaneously lyse 4T1-12B target cells, suggesting that a loss of TSLP function would not enhance anti-tumor immunity mediated through a similar mechanism. Because others had already shown that a CD8+ T cell-mediated response to 4T1 tumor cells does not develop in the 4T1 model [60], we focused on

characterizing the cytotoxic response that is mediated largely by natural killer (NK) cells. Furthermore, there would have been insufficient time for cytotoxic T cells to become sensitized to 4T1-12B during the 4-hour incubation period in this experiment, which was aimed at investigating the *de novo* response.

When we began to compare primary tumor growth in WT and TSLPR$^{-/-}$ mice, it became clear that primary tumors developed less often in TSLPR$^{-/-}$ mice (Table 1). When primary tumors were established, they grew more slowly for a period of time in TSLPR$^{-/-}$ mice (Fig. 6). Olkhanud *et al.* have published similar findings since our study began[33].

TSLP responsiveness also played a role in metastasis to the lung and brain in tumor-bearing mice. In the lung, the median the level of metastasis in mice that had reached their humane endpoint was lower and more consistent in TSLPR$^{-/-}$ mice than in WT mice (Fig. 7), confirming the results of a previously published report and supporting our guiding hypothesis [33]. However, the mechanism by which TSLP promotes tumor metastasis has not yet been described.

The median level of metastasis in the brains of tumor-bearing TSLPR$^{-/-}$ mice was significantly higher than WT mice (Fig. 8). This novel finding was unexpected, and it is noted that the overall levels of metastasis in the brains of mice in both groups was considerably lower than the level observed in the lungs. The reasons for this are unknown but it is possible that the intrinsic properties of the blood-brain barrier (BBB) inhibit the entry of blood-borne 4T1-12B cells into central nervous system in (CNS) in tumor-bearing WT mice. Since the anti-tumor response is shifted towards Th1 immunity in TSLPR$^{-/-}$ mice, it is possible that there is some bystander injury to the BBB that facilitates the movement of 4T1-12B cells across the BBB and into the brain more

readily. Others have shown that that IFNγ and other cytokines characteristic of Th1 immunity increase BBB permeability and enhance damage to the CNS, lending credence to this idea [137-140].

Having observed some differences in the course of the disease in WT and TSLPR$^{-/-}$ mice, we wished to compare the levels of cytotoxicity directed against 4T1-12B tumor cells by splenocytes from tumor-bearing mice. We could not detect a cytotoxic response to the tumor cells in either WT or TSLPR$^{-/-}$ mice with tumors (Table 2), which is consistent with the *de novo* response that we had observed. Interestingly, the levels of YAC-1-directed lysis were also lower in both groups of tumor-bearing mice than in control mice. It was recently shown in a study using the 4T1 model that the cytotoxic response to target cells that are normally sensitive to NK cell-mediated killing, such as YAC-1, is suppressed by modulating prostaglandins, which play a role in mediating inflammation and can modulate NK cell function [141].

The results from our assays for IFN-γ and IL-4 indicate that the cytokine profile in cultures of splenocytes from tumor-bearing TSLPR$^{-/-}$ mice was shifted away from Th2 immunity towards a Th1-type of profile (Fig. 9), providing further support for our hypothesis. We postulate that this is an induced Th1 response, rather than a depletion of Th2 cells, as the cell counts from spleens from tumor-bearing WT and TSLPR$^{-/-}$ mice were roughly the same (data not shown).

Cultures of primary tumors from tumor-bearing mice that had reached humane endpoint contained TSLP but there was no difference in the concentrations seen in tumor cultures from WT or TSLPR$^{-/-}$ mice (Fig. 10). The concentration of IL-12(p40) was

significantly higher in tumors from TSLPR$^{-/-}$ mice than in WT mice, suggesting that the local immune response in the tumor microenvironment is shifted towards Th1 immunity.

As an alternative approach to testing our hypothesis, we performed a pilot experiment in which we treated WT mice with a mouse anti-TSLP neutralizing antibody (muM702) *in vivo*. This antibody had been used to demonstrate a role for TSLP in other models of disease such as colitis and intestinal helminth infection[123]. This treatment did not significantly affect primary tumor establishment (Table 3) or primary tumor growth in WT mice (Fig. 11A). Interestingly, there was a trend toward enhanced primary tumor growth in antibody-treated WT mice. The only beneficial effect that we observed in this group was that the level of metastasis to the lungs was significantly lower (Fig. 12A). In this pilot experiment, we also treated TSLPR$^{-/-}$ mice, to see if some of the effects that we had previously seen in these mice could be further enhanced by the antibody treatment. In TSLPR$^{-/-}$ mice, the antibody treatment did not result in any significant differences in the number of mice that established a primary tumor (Table 4), the primary tumor diameters observed (Fig. 11B) or the levels of metastasis to the lung (Fig. 12B) or brain (Figure 13B). It is important to note that this experiment was not optimized, so differences that did not achieve significance in this experiment may achieve significance in an optimized study. One important question that would need to be addressed is whether the antibody levels in the tumor microenvironment reach levels that are high enough to neutralize the local concentration of TSLP. We did not pursue this aspect of the project further but instead decided to focus on completing other aspects of our study. If we were to continue with this part of the study, it would be important to use larger

numbers of mice and include control groups in which the mice were treated with an appropriate isotype control antibody.

Since the start of our study, others have shown that TSLP is expressed in human breast cancer cell lines and in tumor cells in human breast cancer tissue [33, 127]. To our knowledge, nothing has yet been reported about TSLP expression in normal breast tissue. When we investigated TSLP expression in tissue microarrays from the Manitoba Breast Tumor Bank we found that both normal glandular epithelium and breast tumor cells stained positively for TSLP. This finding confirms that TSLP is expressed in breast cancer cells in humans and further shows that it is also expressed in normal breast epithelial cells. As TSLP expression in the tumor tissue and normal tissue was not quantified, it is impossible to know if tumor epithelial cells are expressing TSLP at higher levels than normal epithelial cells. Further studies on tumor tissue from a range of tumor types, grades and patient ages are required to fully assess the function of TSLP in normal and malignant breast tissue in humans.

Near the end of this study, we made some unexpected observations regarding housing conditions and the 4T1 mouse mammary tumor model. In September 2012, the University of Manitoba Central Animal Care Services implemented a new rodent housing system in which mice were maintained in individually ventilated cages (IVC) with a HEPA-filtered air supply. This was done to comply with new standards set by the Canadian Council on Animal Care and is aimed at minimizing the exposure of staff to airborne allergens present in the facility. We found that there was no difference in the number of WT mice that established primary tumors in IVC and conventional housing (Table 5). Although more of the $TSLPR^{-/-}$ mice housed in IVC conditions developed

primary tumors than the conventionally-housed counterparts, the difference was not significant (Table 6). There was a trend towards smaller primary tumor diameters in WT mice in IVC housing compared to conventional housing from day 25 onward, and the difference was significant on day 35 (Fig. 15A). This suggests that inhaled antigens in conventional housing promote primary tumor growth in WT mice. The differences in the primary tumor diameters were not significant in $TSLPR^{-/-}$ mice housed in IVC conditions or conventional housing (Fig. 15B). When we compared the concentrations of IFNγ, IL-4 and IL-10, we found that the levels were markedly lower in both WT and $TSLPR^{-/-}$ mice housed that had been housed in IVC conditions at nearly all of the time points tested (Fig. 16). This cannot be explained by a reduction in TSLP expression by the primary tumor since there were no significant differences in the concentrations of TSLP in primary tumor cultures from either WT or $TSLPR^{-/-}$ mice that had been housed in either IVC conditions or conventional cages (Fig. 17). The shift away from Th2 immunity in $TSLPR^{-/-}$ that we had observed with conventional housing was not seen in the mice housed in IVC conditions (ANOVA, $p>0.05$ for the three cytokines tested). Collectively, these observations show an important role for the environment in promoting the progression of breast cancer. A possible explanation for this finding is that epidemiological studies of human breast cancer show that there is a strong association between smoking and the development of breast cancer [142, 143] and that women living in areas with higher ambient levels of ammonia, nitrogen oxides, CO and SO_2 have a higher incidence of breast cancer [144-148]. Furthermore, IVC housing results in lower levels of ammonia exposure in the cages [149]. In the tumor microenvironment, ammonia, which is a byproduct of glutaminolysis, has been shown to induce autophagy

and condition a tumor-promoting microenvironment [150, 151]. This may, in part, explain our finding that tumors grew more slowly in WT mice maintained in IVC conditions. Greater numbers of mice and additional experiments would be needed to determine the precise mechanisms involved.

V. SIGNIFICANCE AND FUTURE DIRECTIONS

Our findings from experiments involving TSLPR$^{-/-}$ mice indicate that the establishment and growth of the primary tumor, as well as metastasis to the lung are diminished somewhat in mice that cannot respond to TSLP. This is associated with a shift away from an immune response that is dominated by Th2 cytokines. Collectively, these results support our central hypothesis. Importantly, they also show that the ability of immune cells to respond to TSLP is not an absolute requirement for these aspects of the disease, as they were still observed, albeit at a lower level, in TSLPR$^{-/-}$ mice. The precise mechanism through which TSLP promotes the development of a permissive microenvironment that facilitates the growth and metastasis of the primary tumor is not known. Our findings suggest that suppression of tumor cell lysis by effector cells is not likely involved.

During the course of our study, another group reported results from a similar study, in which they also used the 4T1 mouse model of breast cancer and TSLPR$^{-/-}$ mice [33]. They showed that both human and mouse breast tumor cell lines produce TSLP, and this was confirmed *in vivo* by examining breast tumor metastasis to the lungs from both human patient biopsy material and lung tissue from tumor-bearing mice. Additionally, they used TSLP-deficient 4T1 cells and TSLPR$^{-/-}$ mice to show that enhances primary tumor growth and lung metastasis. The cytokines they examined were characteristic of Th2 immunity, and they showed a reduction in Th2 cytokines when mice were implanted with TSLP-deficient 4T1 cells. Our study confirms several of these findings but also includes new findings regarding the role of TSLP in the establishment of the primary tumor. Our observation that the absence of TSLP responsiveness is

associated with increased metastasis to the brain is also novel. The cytokine data in our study not only examines the immune response in terms of Th2 cytokines, but also measures Th1 cytokines in tumor-bearing WT and TSLPR$^{-/-}$ mice. Other unique aspects of our study were the analysis of cytotoxicity directed against the tumor cells and the report of TSLP expression in normal human breast epithelium.

Further characterization of the mechanism through which TSLP is able to promote the development of a permissive microenvironment requires further investigation. This is important with respect to our understanding of anti-tumor responses in breast cancer and in the development of any new treatments in which TSLP is targeted therapeutically. One possible explanation for the results obtained from these studies is that TSLP and other factors are working synergistically to remodel the tumor microenvironment, similar to how TSLP contributes to airway remodeling in allergic asthma [152]. As described in the introduction, 4T1 cells express T_{reg} and monocyte recruitment factors and activate angiogenesis and lymphangiogenesis pathways, which contribute to remodeling of the tumor environment [44]. It is possible that angiogenic cytokines secreted by 4T1 cells initiate remodeling of the tumor microenvironment, while secreted TSLP serves to enhance further environmental remodeling by promoting a Th2 immune response.

The TSLP neutralization experiments require further study. The distribution pattern of the antibody in tumor-bearing mice is currently unknown. This could be investigated by injecting mice with labeled antibody and tracking its distribution with an *in vivo* imaging system. This approach could be used in concert with alternative routes of antibody delivery (e.g. intratumoral injection) to ensure that free TSLP is effectively

neutralized in the tumor microenvironment. *In vitro* experiments using cultures of dissociated primary tumors and various concentrations of anti-TSLP antibody might also help to determine the physiological concentration of antibody required to neutralize the tumor-derived TSLP.

The 4T1 mouse mammary tumor model has been extensively utilized in the field of TSLP biology and the role of TSLP in the pathogenesis of cancer. It's value as a model system is that it is a fully immunocompetent model that requires minimal manipulation in order to obtain results[45]. However, each model has its strengths and weaknesses. Therefore, it is important to evaluate any important concept in multiple experimental model systems in order to completely understand the mechanistic underpinnings of any biological phenomenon. To further understand the immunological basis of the role TSLP plays in inhibiting anti-tumor immunity, further studies are required in models that mimic the various clinical subtypes and molecular phenotypes of human breast cancer [153]. For example, the polyoma middle T antigen mouse model mimics $HER2^+$ breast cancer, and there are numerous transgenic mouse models to mimic ER^+ luminal breast cancer (reviewed by Holliday and Speirs) [154].

A beneficial addition to this study would be a comprehensive study comparing TSLP expression in human breast cancer. A study of this nature would examine TSLP expression in the major clinical breast cancer subtypes and stages of the disease, as well as examining normal breast epithelial cells from the same patient. Patterns found in TSLP expression would help to establish the prognostic value of TSLP in human breast cancer.

There is no question that breast cancer is a complex disease. Our findings, as well as recent findings from other investigators provide support for the idea that TSLP helps to

create a permissive microenvironment for mammary carcinoma. As such, they provide the rationale for new studies aimed at further evaluating the mechanisms of action for TSLP, as well as its prognostic value in human breast cancer.

VI. REFERENCES

1. Curtis, C., et al., *The genomic and transcriptomic architecture of 2000 breast tumours reveals novel subgroups.* Nature, 2012. **486**: p. 346-52.
2. Statistics, C.C.S.s.S.C.o.C., *Canadian Cancer Statistics 2012*, 2012, Canadian Cancer Society: Toronto, ON.
3. Claus, E.B., N. Risch, and W.D. Thompson, *Autosomal dominant inheritance of early-onset breast cancer. Implications for risk prediction.* Cancer, 1994. **73**(3): p. 643-51.
4. Blackwood, M.A. and B.L. Weber, *BRCA1 and BRCA2: from molecular genetics to clinical medicine.* J Clin Oncol, 1998. **16**(5): p. 1969-77.
5. *Cancer risks in BRCA2 mutation carriers. The Breast Cancer Linkage Consortium.* J Natl Cancer Inst, 1999. **91**(15): p. 1310-6.
6. Fishman, A., *The effects of parity, breastfeeding, and infertility treatment on the risk of hereditary breast and ovarian cancer: a review.* Int J Gynecol Cancer, 2010. **20**(11 Suppl 2): p. S31-3.
7. Chlebowski, R.T. and G.L. Anderson, *Changing concepts: Menopausal hormone therapy and breast cancer.* J Natl Cancer Inst, 2012. **104**(7): p. 517-27.
8. Simpson, J.F., et al., *Prognostic value of histologic grade and proliferative activity in axillary node-positive breast cancer: results from the Eastern Cooperative Oncology Group Companion Study, EST 4189.* J Clin Oncol, 2000. **18**(10): p. 2059-69.
9. Rouzier, R., et al., *Breast cancer molecular subtypes respond differently to preoperative chemotherapy.* Clin Cancer Res, 2005. **11**(16): p. 5678-85.
10. Eroles, P., et al., *Molecular biology in breast cancer: intrinsic subtypes and signaling pathways.* Cancer Treat Rev, 2012. **38**(6): p. 698-707.
11. Rakha, E.A. and S. Chan, *Metastatic triple-negative breast cancer.* Clin Oncol (R Coll Radiol), 2011. **23**(9): p. 587-600.
12. Nandini, D., B.R. Smith, and B. Leyland-Jones, *Targeting Basal-Like Breast Cancers.* Curr Drug Targets, 2012.
13. Nielsen, T.O., et al., *Immunohistochemical and clinical characterization of the basal-like subtype of invasive breast carcinoma.* Clin Cancer Res, 2004. **10**(16): p. 5367-74.
14. Fulford, L.G., et al., *Basal-like grade III invasive ductal carcinoma of the breast: patterns of metastasis and long-term survival.* Breast Cancer Res, 2007. **9**(1): p. R4.
15. Spano, D., et al., *Dipyridamole prevents triple-negative breast-cancer progression.* Clin Exp Metastasis, 2013. **30**(1): p. 47-68.
16. Sun, X., et al., *"Iron-saturated" bovine lactoferrin improves the chemotherapeutic effects of tamoxifen in the treatment of basal-like breast cancer in mice.* BMC Cancer, 2012. **12**: p. 591.
17. Verbrugge, I., et al., *Radiotherapy increases the permissiveness of established mammary tumors to rejection by immunomodulatory antibodies.* Cancer Res, 2012. **72**(13): p. 3163-74.

18. Zardavas, D., I. Bozovic-Spasojevic, and E. de Azambuja, *Dual human epidermal growth factor receptor 2 blockade: another step forward in treating patients with human epidermal growth factor receptor 2-positive breast cancer.* Curr Opin Oncol, 2012.
19. Cicalese, A., et al., *The tumor suppressor p53 regulates polarity of self-renewing divisions in mammary stem cells.* Cell, 2009. **138**(6): p. 1083-95.
20. Kauraniemi, P. and A. Kallioniemi, *Activation of multiple cancer-associated genes at the ERBB2 amplicon in breast cancer.* Endocr Relat Cancer, 2006. **13**(1): p. 39-49.
21. Sorlie, T., et al., *Gene expression patterns of breast carcinomas distinguish tumor subclasses with clinical implications.* Proc Natl Acad Sci U S A, 2001. **98**(19): p. 10869-74.
22. Perou, C.M., et al., *Molecular portraits of human breast tumours.* Nature, 2000. **406**(6797): p. 747-52.
23. Carey, L.A., et al., *Race, breast cancer subtypes, and survival in the Carolina Breast Cancer Study.* JAMA, 2006. **295**(21): p. 2492-502.
24. Goldhirsch, A., et al., *Strategies for subtypes--dealing with the diversity of breast cancer: highlights of the St. Gallen International Expert Consensus on the Primary Therapy of Early Breast Cancer 2011.* Ann Oncol, 2011. **22**(8): p. 1736-47.
25. Calza, S., et al., *Intrinsic molecular signature of breast cancer in a population-based cohort of 412 patients.* Breast Cancer Res, 2006. **8**(4): p. R34.
26. Dawood, S., et al., *Defining breast cancer prognosis based on molecular phenotypes: results from a large cohort study.* Breast Cancer Res Treat, 2011. **126**(1): p. 185-92.
27. Lund, M.J., et al., *Age/race differences in HER2 testing and in incidence rates for breast cancer triple subtypes: a population-based study and first report.* Cancer, 2010. **116**(11): p. 2549-59.
28. Dexter, D.L., et al., *Heterogeneity of tumor cells from a single mouse mammary tumor.* Cancer Res, 1978. **58**(3174-3181).
29. Aslakson, C.J. and F.R. Miller, *Selective events in the metastatic process defined by analysis of the sequential dissemination of subpopulations of a mouse mammary tumor. .* Cancer Res, 1992. **52**: p. 1399-1405.
30. Heppner, G.H., et al., *Heterogeneity in drug sensitivity among tumor cell subpopulations of a single mammary tumor.* Cancer Res, 1978. **38**(11 Pt 1): p. 3758-63.
31. Lelekakis, M., et al., *A novel orthotopic model of breast cancer metastasis to bone.* Clin Exp Metastasis, 1999. **17**(2): p. 163-70.
32. Kurt, R.A., et al., *Chemokine receptor desensitization in tumor-bearing mice.* Cell Immunol, 2001. **207**(2): p. 81-8.
33. Olkhanud, P.B., et al., *Thymic stromal lymphopoietin is a key mediator of breast cancer progression.* J Immunol, 2011. **186**(10): p. 5656-62.
34. Adler, E.P., et al., *A dual role for tumor-derived chemokine RANTES (CCL5).* Immunol Lett, 2003. **90**(2-3): p. 187-94.
35. Vitiello, P.F., et al., *Impact of tumor-derived CCL2 on T cell effector function.* Immunol Lett, 2004. **91**(2-3): p. 239-45.

36. DuPre, S.A. and K.W. Hunter, Jr., *Murine mammary carcinoma 4T1 induces a leukemoid reaction with splenomegaly: association with tumor-derived growth factors.* Exp Mol Pathol, 2007. **82**(1): p. 12-24.
37. DuPre, S.A., D. Redelman, and K.W. Hunter, Jr., *The mouse mammary carcinoma 4T1: characterization of the cellular landscape of primary tumours and metastatic tumour foci.* Int J Exp Pathol, 2007. **88**(5): p. 351-60.
38. McEarchern, J.A., et al., *Invasion and metastasis of a mammary tumor involves TGF-beta signaling.* Int J Cancer, 2001. **91**(1): p. 76-82.
39. Reiss, M. and M.H. Barcellos-Hoff, *Transforming growth factor-beta in breast cancer: a working hypothesis.* Breast Cancer Res Treat, 1997. **45**(1): p. 81-95.
40. Roberts, A.B., et al., *Transforming growth factor type beta: rapid induction of firbrosis and angiogenesis in vivo and stimulation of collagen formation in vitro.* PNAS, 1986. **83**(12): p. 4167-71.
41. Albo, D., et al., *Thrombospondin-1 and transforming growth factor-beta l promote breast tumor cell invasion through up-regulation of the plasminogen/plasmin system.* Surgery, 1997. **122**(2): p. 493-9; discussion 499-500.
42. Arteaga, C.L., et al., *Anti-transforming growth factor (TGF)-beta antibodies inhibit breast cancer cell tumorigenicity and increase mouse spleen natural killer cell activity. Implications for a possible role of tumor cell/host TGF-beta interactions in human breast cancer progression.* J Clin Invest, 1993. **92**(6): p. 2569-76.
43. Park, J.A., et al., *Expression of an antisense transforming growth factor-beta1 transgene reduces tumorigenicity of EMT6 mammary tumor cells.* Cancer Gene Ther, 1997. **4**(1): p. 42-50.
44. Tao, K., et al., *Imagable 4T1 model for the study of late stage breast cancer.* BMC Cancer, 2008. **8**: p. 228.
45. Pulaski, B.A. and S. Ostrand-Rosenberg, *Mouse 4T1 Breast Tumor Model.* Curr Prot Immunol, 2000: p. 20.2.1-16.
46. O'Garra, A., *Cytokines induce the development of functionally heterogeneous T helper cell subsets.* Immunity, 1998. **8**(3): p. 275-83.
47. Ariga, H., et al., *Instruction of naive CD4+ T-cell fate to T-bet expression and T helper 1 development: roles of T-cell receptor-mediated signals.* Immunology, 2007. **122**(2): p. 210-21.
48. Manetti, R., et al., *Natural killer cell stimulatory factor (interleukin 12 [IL-12]) induces T helper type 1 (Th1)-specific immune responses and inhibits the development of IL-4-producing Th cells.* J Exp Med, 1993. **177**(4): p. 1199-204.
49. Wan, Y.Y., *Multi-tasking of helper T cells.* Immunology, 2010. **130**(2): p. 166-71.
50. Nawijn, M.C., et al., *Enforced expression of GATA-3 in transgenic mice inhibits Th1 differentiation and induces the formation of a T1/ST2-expressing Th2-committed T cell compartment in vivo.* J Immunol, 2001. **167**(2): p. 724-32.
51. Kaplan, M.H., et al., *Stat6 is required for mediating responses to IL-4 and for development of Th2 cells.* Immunity, 1996. **4**(3): p. 313-9.
52. Takeda, K., et al., *Essential role of Stat6 in IL-4 signalling.* Nature, 1996. **380**(6575): p. 627-30.

53. Noben-Trauth, N., et al., *An interleukin 4 (IL-4)-independent pathway for CD4+ T cell IL-4 production is revealed in IL-4 receptor-deficient mice.* Proc Natl Acad Sci U S A, 1997. **94**(20): p. 10838-43.
54. Lebman, D.A. and R.L. Coffman, *Interleukin 4 causes isotype switching to IgE in T cell-stimulated clonal B cell cultures.* J Exp Med, 1988. **168**(3): p. 853-62.
55. Kobayashi, M., et al., *A pathogenic role of Th2 cells and their cytokine products on the pulmonary metastasis of murine B16 melanoma.* J Immunol, 1998. **160**(12): p. 5869-73.
56. Bellone, G., et al., *Tumor-associated transforming growth factor-beta and interleukin-10 contribute to a systemic Th2 immune phenotype in pancreatic carcinoma patients.* Am J Pathol, 1999. **155**(2): p. 537-47.
57. Nishimura, T., et al., *The critical role of Th1-dominant immunity in tumor immunology.* Cancer Chemother Pharmacol, 2000. **46 Suppl**: p. S52-61.
58. Terabe, M., et al., *NKT cell-mediated repression of tumor immunosurveillance by IL-13 and the IL-4R-STAT6 pathway.* Nat Immunol, 2000. **1**(6): p. 515-20.
59. Smyth, M.J., et al., *Differential tumor surveillance by natural killer (NK) and NKT cells.* J Exp Med, 2000. **191**(4): p. 661-8.
60. Ostrand-Rosenberg, S., M.H. Grusby, and V.K. Clements, *Cutting Edge: STAT6-deficient mice have enhanced tumor immunity to primary and metastatic mammary carcinoma.* J Immunol, 2000. **165**: p. 6015-6019.
61. Thakur, A., et al., *A Th1 cytokine-enriched microenvironment enhances tumor killing by activated T cells armed with bispecific antibodies and inhibits the development of myeloid-derived suppressor cells.* Cancer Immunol Immunother, 2012. **61**(4): p. 497-509.
62. Nunez, S., et al., *Th17 cells contribute to anti-tumor immunity and promote the recruitment of th1 cells to the tumor.* Immunology, 2012.
63. Gately, M.K., D.E. Wilson, and H.L. Wong, *Synergy between recombinant interleukin 2 (rIL 2) and IL 2-depleted lymphokine-containing supernatants in facilitating allogeneic human cytolytic T lymphocyte responses in vitro.* J Immunol, 1986. **136**(4): p. 1274-82.
64. Wang, C., et al., *Characterization of murine macrophages from bone marrow, spleen and peritoneum.* BMC Immunol, 2013. **14**(1): p. 6.
65. Ladoire, S., et al., *T-bet expression in intratumoral lymphoid structures after neoadjuvant trastuzumab plus docetaxel for HER2-overexpressing breast carcinoma predicts survival.* Br J Cancer, 2011. **105**(3): p. 366-71.
66. Oldford, S.A., et al., *Tumor cell expression of HLA-DM associates with a Th1 profile and predicts improved survival in breast carcinoma patients.* Int Immunol, 2006. **18**(11): p. 1591-602.
67. Bunt, S.K., et al., *Inflammation induces myeloid-derived suppressor cells that facilitate tumor progression.* J Immunol, 2006. **176**(1): p. 284-90.
68. Bunt, S.K., et al., *Reduced inflammation in the tumor microenvironment delays the accumulation of myeloid-derived suppressor cells and limits tumor progression. .* Cancer Res, 2007. **67**(20): p. 10019-10026.
69. Obermajer, N., et al., *PGE(2)-driven induction and maintenance of cancer-associated myeloid-derived suppressor cells.* Immunol Invest, 2012. **41**(6-7): p. 635-57.

70. Meyer, C., et al., *Chronic inflammation promotes myeloid-derived suppressor cell activation blocking antitumor immunity in transgenic mouse melanoma model.* Proc Natl Acad Sci U S A, 2011. **108**(41): p. 17111-6.
71. Ohki, S., et al., *Circulating myeloid-derived suppressor cells are increased and correlate to immune suppression, inflammation and hypoproteinemia in patients with cancer.* Oncol Rep, 2012. **28**(2): p. 453-8.
72. Sawant, A., et al., *Depletion of plasmacytoid dendritic cells inhibits tumor growth and prevents bone metastasis of breast cancer cells.* J Immunol, 2012. **189**(9): p. 4258-65.
73. Annacker, O., et al., *CD25+ CD4+ T cells regulate the expansion of peripheral CD4 T cells through the production of IL-10.* J Immunol, 2001. **166**(5): p. 3008-18.
74. Chen, X., Y. Du, and Z. Huang, *CD4+CD25+ Treg derived from hepatocellular carcinoma mice inhibits tumor immunity.* Immunol Lett, 2012. **148**(1): p. 83-9.
75. Chaput, N., et al., *Regulatory T cells prevent CD8 T cell maturation by inhibiting CD4 Th cells at tumor sites.* J Immunol, 2007. **179**(8): p. 4969-78.
76. Chen, L., et al., *Rejection of metastatic 4T1 breast cancer by attenuation of Treg cells in combination with immune stimulation.* Mol Ther, 2007. **15**(12): p. 2194-202.
77. Arase, H., N. Arase, and T. Saito, *Interferon gamma production by natural killer (NK) cells and NK1.1+ T cells upon NKR-P1 cross-linking.* J Exp Med, 1996. **183**(5): p. 2391-6.
78. Kajitani, K., et al., *Mechanistic analysis of the antitumor efficacy of human natural killer cells against breast cancer cells.* Breast Cancer Res Treat, 2012. **134**(1): p. 139-55.
79. Mamessier, E., et al., *Human breast cancer cells enhance self tolerance by promoting evasion from NK cell antitumor immunity.* J Clin Invest, 2011. **121**(9): p. 3609-22.
80. Rook, A.H., et al., *Effects of transforming growth factor beta on the functions of natural killer cells: depressed cytolytic activity and blunting of interferon responsiveness.* J Immunol, 1986. **136**(10): p. 3916-20.
81. Nam, J.S., et al., *Transforming growth factor beta subverts the immune system into directly promoting tumor growth through interleukin-17.* Cancer Res, 2008. **68**(10): p. 3915-23.
82. Ennis, C., *Why I'm feeling so crabby about cancer conspiracy theories*, in *Occam's Corner* 2012, The Guardian: http://www.guardian.co.uk/science/occams-corner/2012/dec/07/cancer-conspiracy-theories.
83. Maenaka, K. and E.Y. Jones, *MHC superfamily structure and the immune system.* Curr Opin Struct Biol, 1999. **9**(6): p. 745-53.
84. Robert, P., et al., *Kinetics and mechanics of two-dimensional interactions between T cell receptors and different activating ligands.* Biophys J, 2012. **102**(2): p. 248-57.

85. Chen, L., et al., *Costimulation of antitumor immunity by the B7 counterreceptor for the T lymphocyte molecules CD28 and CTLA-4.* Cell, 1992. **71**(7): p. 1093-102.
86. Mallick, A., et al., *Neem leaf glycoprotein activates CD8(+) T cells to promote therapeutic anti-tumor immunity inhibiting the growth of mouse sarcoma.* PLoS One, 2013. **8**(1): p. e47434.
87. Brown, M.D., et al., *Loss of antigen cross-presentation after complete tumor resection is associated with the generation of protective tumor-specific CD8(+) T-cell immunity.* Oncoimmunology, 2012. **1**(7): p. 1084-1094.
88. Elliott, J.M. and W.M. Yokoyama, *Unifying concepts of MHC-dependent natural killer cell education.* Trends Immunol, 2011. **32**(8): p. 364-72.
89. Karre, K., et al., *Selective rejection of H-2-deficient lymphoma variants suggests alternative immune defence strategy.* Nature, 1986. **319**(6055): p. 675-8.
90. Belanger, S., et al., *Impaired natural killer cell self-education and "missing-self" responses in Ly49-deficient mice.* Blood, 2012. **120**(3): p. 592-602.
91. Garcia-Lora, A., I. Algarra, and F. Garrido, *MHC class I antigens, immune surveillance, and tumor immune escape.* J Cell Physiol, 2003. **195**(3): p. 346-55.
92. Villalba, M., et al., *From tumor cell metabolism to tumor immune escape.* Int J Biochem Cell Biol, 2012.
93. Dunn, G.P., L.J. Old, and R.D. Schreiber, *The immunobiology of cancer immunosurveillance and immunoediting.* Immunity, 2004. **21**(2): p. 137-48.
94. Quentmeier, H., et al., *Cloning of human thymic stromal lymphopoietin (TSLP) and signaling mechanisms leading to proliferation.* Leukemia, 2001. **15**(8): p. 1286-92.
95. Friend, S.L., et al., *A thymic stromal cell line supports in vitro development of surface IgM+ B cells and produces a novel growth factor affecting B and T lineage cells.* Exp Hematol, 1994. **22**(3): p. 321-8.
96. Reche, P.A., et al., *Human thymic stromal lymphopoietin preferentially stimulates myeloid cells.* J Immunol, 2001. **167**(1): p. 336-43.
97. He, R. and R.S. Geha, *Thymic stromal lymphopoietin.* Ann N Y Acad Sci, 2010. **1183**: p. 13-24.
98. Soumelis, V., et al., *Human epithelial cells trigger dendritic cell mediated allergic inflammation by producing TSLP.* Nat Immunol, 2002. **3**(7): p. 673-80.
99. Zhang, K., et al., *Constitutive and inducible thymic stromal lymphopoietin expression in human airway smooth muscle cells: role in chronic obstructive pulmonary disease.* Am J Physiol Lung Cell Mol Physiol, 2007. **293**(2): p. L375-82.
100. Kashyap, M., et al., *Thymic stromal lymphopoietin is produced by dendritic cells.* J Immunol, 2011. **187**(3): p. 1207-11.
101. Redhu, N.S. and A.S. Gounni, *Function and mechanisms of TSLP/TSLPR complex in asthma and COPD.* Clin Exp Allergy, 2012. **42**: p. 994-1005.
102. Park, L., et al., *Cloning of the Murine Thymic Stromal Lymphopoietin (Tslp) Receptor.* J Exp Med, 2000. **192**(5): p. 569-670.

103. Roan, F., et al., *The multiple facets of thymic stromal lymphopoietin (TSLP) during allergic inflammation and beyond.* J Leukoc Biol, 2012. **91**(6): p. 877-86.
104. Tonozuka, Y., et al., *Molecular cloning of a human novel type I cytokine receptor related to delta1/TSLPR.* Cytogenet Cell Genet, 2001. **93**(1-2): p. 23-5.
105. Isaksen, D.E., et al., *Uncoupling of proliferation and Stat5 activation in thymic stromal lymphopoietin-mediated signal transduction.* J Immunol, 2002. **168**(7): p. 3288-94.
106. Rochman, Y., et al., *Thymic stromal lymphopoietin-mediated STAT5 phosphorylation via kinases JAK1 and JAK2 reveals a key difference from IL-7-induced signaling.* Proc Natl Acad Sci U S A, 2010. **107**(45): p. 19455-60.
107. Lu, N., et al., *TSLP and IL-7 use two different mechanisms to regulate human CD4+ T cell homeostasis.* J Exp Med, 2009. **206**(10): p. 2111-9.
108. Arima, K., et al., *Distinct signal codes generate dendritic cell functional plasticity.* Sci Signal, 2010. **3**(105): p. ra4.
109. Ziegler, S.F. and D. Artis, *Sensing the outside world: TSLP regulates barrier immunity.* Nat Immunol, 2010. **11**(4): p. 289-93.
110. Liu, Y.J., *Thymic stromal lymphopoietin and OX40 ligand pathway in the initiation of dendritic cell-mediated allergic inflammation.* J Allergy Clin Immunol, 2007. **120**(2): p. 238-44.
111. Li, H., et al., *Increased prevalence of regulatory T cells in the lung cancer microenvironment: a role of thymic stromal lymphopoietin.* Cancer Immunol Immunother, 2011. **60**(11): p. 1587-96.
112. Ito, T., et al., *TSLP-activated dendritic cells induce an inflammatory T helper type 2 cell response through OX40 ligand.* J Exp Med, 2005. **202**(9): p. 1213-23.
113. Rochman, I., et al., *Cutting edge: direct action of thymic stromal lymphopoietin on activated human CD4+ T cells.* J Immunol, 2007. **178**(11): p. 6720-4.
114. Omori, M. and S. Ziegler, *Induction of IL-4 expression in CD4(+) T cells by thymic stromal lymphopoietin.* J Immunol, 2007. **178**(3): p. 1396-404.
115. Bieber, T., *Atopic Dermatitis.* N Engl J Med, 2008. **358**(14): p. 1483-94.
116. Yoo, J., et al., *Spontaneous atopic dermatitis in mice expressing an inducible thymic stromal lymphopoietin transgene specifically in the skin.* J Exp Med, 2005. **202**(4): p. 541-9.
117. Zhou, B., et al., *Thymic stromal lymphopoietin as a key initiator of allergic airway inflammation in mice.* Nat Immunol, 2005. **6**(10): p. 1047-53.
118. Redhu, N.S., et al., *IgE induces transcriptional regulation of thymic stromal lymphopoietin in human airway smooth muscle cells.* J Allergy Clin Immunol, 2011. **128**(4): p. 892-896 e2.
119. Al-Shami, A., et al., *A role for TSLP in the development of inflammation in an asthma model.* J Exp Med, 2005. **202**(6): p. 829-39.
120. Headley, M.B., et al., *TSLP conditions the lung immune environment for the generation of pathogenic innate and antigen-specific adaptive immune responses.* J Immunol, 2009. **182**(3): p. 1641-7.

121. Ying, S., et al., *Thymic stromal lymphopoietin expression is increased in asthmatic airways and correlates with expression of Th2-attracting chemokines and disease severity.* J Immunol, 2005. **174**(12): p. 8183-90.
122. Nishiura, H., et al., *Increased susceptibility to autoimmune gastritis in thymic stromal lymphopoietin receptor-deficient mice.* J Immunol, 2012. **188**(1): p. 190-7.
123. Taylor, B.C., et al., *TSLP regulates intestinal immunity and inflammation in mouse models of helminth infection and colitis.* J Exp Med, 2009. **206**(3): p. 655-67.
124. Liu, Y.J., *Thymic stromal lymphopoietin: master switch for allergic inflammation.* J Exp Med, 2006. **203**(2): p. 269-73.
125. Qin, Y., et al., *Constitutive abberant endogenous interleukin-1 facilitates inflammation and growth in human melanoma.* Mol Cancer Res, 2011. **9**(11): p. 1537-50.
126. De Monte, L., et al., *Intratumor T helper type 2 cell infiltrate correlates with cancer-associated fibroblast thymic stromal lymphopoietin production and reduced survival in pancreatic cancer.* J Exp Med, 2011. **208**(3): p. 469-78.
127. Pedroza-Gonzalez, A., et al., *Thymic stromal lymphopoietin fosters human breast tumor growth by promoting type 2 inflammation.* J Exp Med, 2011. **208**(3): p. 479-90.
128. Di Piazza, M., et al., *Loss of Cutaneous TSLP-Dependent Immune Responses Skews the Balance of Inflammation from Tumor Protective to Tumor Promoting.* Cancer Cell, 2012. **22**(4): p. 479-93.
129. Klangsinsirikul, P. and N.H. Russell, *Peripheral blood stem cell harvests from G-CSF-stimulated donors contain a skewed Th2 CD4 phenotype and a predominance of type 2 dendritic cells.* Exp Hematol, 2002. **30**(5): p. 495-501.
130. Al-Shami, A., et al., *A role for thymic stromal lymphopoietin in CD4(+) T cell development.* J Exp Med, 2004. **200**(2): p. 159-68.
131. Petersson, M., et al., *Constitutive IL-10 production accounts for the high NK sensitivity, low MHC class I expression, and poor transporter associated with antigen processing (TAP)-1/2 function in the prototype NK target YAC-1.* J Immunol, 1998. **161**(5): p. 2099-105.
132. Ellison, C.A., et al., *Palifermin mediates immunoregulatory effects in addition to its cytoprotective effects in mice with acute graft-versus-host disease.* J Clin Immunol, 2008. **28**(5): p. 600-15.
133. Pross, H.F. and J.A. Maroun, *The standardization of NK cell assays for use in studies of biological response modifiers.* J Immunol Methods, 1984. **68**(1-2): p. 235-49.
134. Manthorpe, M., et al., *Gene therapy by intramuscular injection of plasmid DNA: Studies on firefly luciferase gene expression in mice.* Human Gene Ther, 1993. **4**: p. 419-431.
135. Watson, P.H., L. Snell, and M. Parisien, *The NCIC-Manitoba Breast Tumor Bank: a resource for applied cancer research.* CMAJ, 1996. **155**(3): p. 281-3.
136. Skliris, G.P., et al., *Expression of oestrogen receptor-beta in oestrogen receptor-alpha negative human breast tumours.* Br J Cancer, 2006. **95**(5): p. 616-26.

137. Lopez-Ramirez, M.A., et al., *Role of caspases in cytokine-induced barrier breakdown in human brain endothelial cells.* J Immunol, 2012. **189**(6): p. 3130-9.
138. Minagar, A. and J.S. Alexander, *Blood-brain barrier disruption in multiple sclerosis.* Mult Scler, 2003. **9**(6): p. 540-9.
139. Schmidt, K.E., et al., *Induction of pro-inflammatory mediators in Plasmodium berghei infected BALB/c mice breaks blood-brain-barrier and leads to cerebral malaria in an IL-12 dependent manner.* Microbes Infect, 2011. **13**(10): p. 828-36.
140. Wong, D., K. Dorovini-Zis, and S.R. Vincent, *Cytokines, nitric oxide, and cGMP modulate the permeability of an in vitro model of the human blood-brain barrier.* Exp Neurol, 2004. **190**(2): p. 446-55.
141. Holt, D.M., et al., *Modulation of host natural killer cell functions in breast cancer via prostaglandin E2 receptors EP2 and EP4.* J Immunother, 2012. **35**(2): p. 179-88.
142. Luo, J., et al., *Association of active and passive smoking with risk of breast cancer among postmenopausal women: a prospective cohort study.* BMJ, 2011. **342**: p. d1016.
143. Johnson, K.C., et al., *Active smoking and secondhand smoke increase breast cancer risk: the report of the Canadian Expert Panel on Tobacco Smoke and Breast Cancer Risk (2009).* Tob Control, 2011. **20**(1): p. e2.
144. Chen, F. and W.F. Bina, *Correlation of white female breast cancer incidence trends with nitrogen dioxide emission levels and motor vehicle density patterns.* Breast Cancer Res Treat, 2012. **132**(1): p. 327-33.
145. Wei, Y., J. Davis, and W.F. Bina, *Ambient air pollution is associated with the increased incidence of breast cancer in US.* Int J Environ Health Res, 2012. **22**(1): p. 12-21.
146. Ranzi, A., et al., *Mortality and morbidity among people living close to incinerators: a cohort study based on dispersion modeling for exposure assessment.* Environ Health, 2011. **10**: p. 22.
147. Crouse, D.L., et al., *Postmenopausal breast cancer is associated with exposure to traffic-related air pollution in Montreal, Canada: a case-control study.* Environ Health Perspect, 2010. **118**(11): p. 1578-83.
148. Mitra, A.K. and F.S. Faruque, *Breast cancer incidence and exposure to environmental chemicals in 82 counties in Mississippi.* South Med J, 2004. **97**(3): p. 259-63.
149. Baumans, V., et al., *Individually ventilated cages: beneficial for mice and men?* Contemp Top Lab Anim Sci, 2002. **41**(1): p. 13-9.
150. Ko, Y.H., et al., *Glutamine fuels a vicious cycle of autophagy in the tumor stroma and oxidative mitochondrial metabolism in epithelial cancer cells: implications for preventing chemotherapy resistance.* Cancer Biol Ther, 2011. **12**(12): p. 1085-97.
151. Marino, G. and G. Kroemer, *Ammonia: a diffusible factor released by proliferating cells that induces autophagy.* Sci Signal, 2010. **3**(124): p. pe19.

152. Chen, Z.G., et al., *Neutralization of TSLP Inhibits Airway Remodeling in a Murine Model of Allergic Asthma Induced by Chronic Exposure to House Dust Mite.* PLoS One, 2013. **8**(1): p. e51268.
153. Borowsky, A.D., *Choosing a mouse model: experimental biology in context--the utility and limitations of mouse models of breast cancer.* Cold Spring Harb Perspect Biol, 2011. **3**(9): p. a009670.
154. Holliday, D.L. and V. Speirs, *Choosing the right cell line for breast cancer research.* Breast Cancer Res, 2011. **13**(4): p. 215.